

Distributed space-time coding for cooperative networks

Sergio Barbarossa

Contract No. R&D N62558-03-M-0814

Final Report

SUMMARY

In this report we show how proper cooperation among radio nodes may provide diversity gain, also for single antenna systems. We consider first the connectivity of a wireless network and show how it can benefit from cooperation. Then, we consider some specific forms of cooperations, based on distributed space-time coding, in both single and multi-user contexts. Finally, we pay a special attention to the case where the final destination has a multi-antenna receiver. In such a case, we may establish a virtual MIMO link between the relays and the final destination, which makes possible to benefit also from the MIMO spatial multiplexing gain.

Report Documentation Page			Form Approved OMB No. 0704-0188	
<p>Public reporting burden for the collection of information is estimated to average 1 hour per response, including the time for reviewing instructions, searching existing data sources, gathering and maintaining the data needed, and completing and reviewing the collection of information. Send comments regarding this burden estimate or any other aspect of this collection of information, including suggestions for reducing this burden, to Washington Headquarters Services, Directorate for Information Operations and Reports, 1215 Jefferson Davis Highway, Suite 1204, Arlington VA 22202-4302. Respondents should be aware that notwithstanding any other provision of law, no person shall be subject to a penalty for failing to comply with a collection of information if it does not display a currently valid OMB control number.</p>				
1. REPORT DATE 05 DEC 2006	2. REPORT TYPE N/A	3. DATES COVERED -		
4. TITLE AND SUBTITLE Distributed Space-Time Coding for Cooperative			5a. CONTRACT NUMBER	
			5b. GRANT NUMBER	
			5c. PROGRAM ELEMENT NUMBER	
6. AUTHOR(S)			5d. PROJECT NUMBER	
			5e. TASK NUMBER	
			5f. WORK UNIT NUMBER	
7. PERFORMING ORGANIZATION NAME(S) AND ADDRESS(ES) Professor Sergio Barbarossa INFOCOM Department University of Rome LA			8. PERFORMING ORGANIZATION REPORT NUMBER	
9. SPONSORING/MONITORING AGENCY NAME(S) AND ADDRESS(ES)			10. SPONSOR/MONITOR'S ACRONYM(S)	
			11. SPONSOR/MONITOR'S REPORT NUMBER(S)	
12. DISTRIBUTION/AVAILABILITY STATEMENT Approved for public release, distribution unlimited				
13. SUPPLEMENTARY NOTES				
14. ABSTRACT				
15. SUBJECT TERMS				
16. SECURITY CLASSIFICATION OF:		17. LIMITATION OF ABSTRACT SAR	18. NUMBER OF PAGES 53	19a. NAME OF RESPONSIBLE PERSON
a. REPORT unclassified	b. ABSTRACT unclassified			

One of the distinguishing features of radio channels is its fading nature. Channel fading has received a considerable attention as it can cause severe performance losses. Since fading is a multiplicative phenomenon, the best way to counteract it is not a simple increase of transmission power. The other major characteristic of radio propagation is its broadcasting nature: The information emitted by a radio source travels in fact in all directions, even though with possibly different amplitudes, depending on the antenna directivity. This means that part of the transmitted energy, a typically scarce resource, is inevitably wasted. To limit such a waste, one should use directive antennas, but sometimes this could be highly impractical, especially on portable handsets, as it requires the use of large antennas (with respect to the transmit wavelength).

The most effective strategy to combat channel fading is diversity. Diversity relies on the existence of more than one path between transmitter and receiver through which the information bits may be conveyed. If the paths are random, but not strongly correlated to each other, one can find optimal strategies to combine the multiple replicas of the received signal in order to minimize the bit error rate (BER). The most known form of diversity is spatial receive diversity, obtainable when the receiver has multiple receive antennas. Nevertheless the last years have witnessed a huge amount of research on methods capable of achieving a spatial diversity even in the case where the receiver has only one antenna, but the transmitter has multiple antennas. In such a case, it is necessary to transmit the data using a particular form of coding that spreads the information bits across the two-dimensional space-time domain, using the so called *space-time coding* [6], [7]. If properly designed, space-time coding guarantees full diversity gain, even in cases where the transmitter does not have any information about the channels.

However, if both transmitters and receivers have only one antenna, it looks like there should be no way to achieve any spatial diversity. Indeed, this is not true, if more radio nodes (relays) contribute to the transmission from one source to the intended destination. In fact, it is precisely the broadcasting nature of radio transmissions that makes possible the propagation of the same information through several relay nodes willing to cooperate with the original source. If the radio nodes that have correctly decoded the same message cooperate with each other to re-transmit the information to the final destination, the overall system may benefit of spatial diversity, even if each radio node has only one antenna. This technical report focuses on this idea and on the ways to achieve diversity through cooperation.

Multihop radio networking is a research field whose study started long time ago (see, e.g. [1] and the

references therein). Some basic theorems on the capacity of relaying networks were established in [2], [8], [14], [15], [4], [5], [3]. Conventional relaying can indeed be seen as a particular form of *distributed space-time coding*, where the same information is transmitted from different (spatial) locations, at different times. From this perspective, relaying can thus be interpreted as a repetition code in the space-time domain. As well known, repetition coding is not the best coding strategy and thus one should achieve a considerable gain by using more sophisticated space-time coding techniques. This form of space-time coding that coordinates the transmission of source and relays is called *distributed* space-time coding. Quite recently, the interest about relaying networks, especially in the form of cooperation among nodes, has increased considerably. One result that sparked great interest was that cooperation among users can increase the capacity in an uplink multiuser channel [16]. A thorough analysis of the diversity gain achievable with cooperation was given in [17], [18], [19], where different distributed cooperation protocols were compared. Cooperation was proved to be very useful to combat shadowing effects, as shown in [20], and it can occur in different forms, as suggested in many recent works, like e.g. [18], [21], [22], [23], [24], [25], [26], [27], [28], [29], [30]. Among all these possibilities, there is the basic idea of using the relays as if they were the antennas of a multi-antenna transmitter. Within this perspective, cooperation induces a *virtual* array between transmitter and receiver. This opens the field to a huge amount of possibilities, provided by all coding methods devised for multi-input/multi-output (MIMO) transceivers. In this more general framework, the relaying problem becomes the problem of mapping the algorithms valid for real MIMO systems into cooperation strategies of a virtual MIMO system.

This technical report is organized as follows. In Section ??, we study the connectivity of a wireless network and show how a single user system can achieve a considerable gain thanks to the cooperation with relay nodes scattered randomly in a given territory. In Section II, we introduce the so called distributed space-time coding (DSTC) strategy, where source and relays transmit in a coordinate manner according to a space-time code distributed among the cooperating nodes. In Section III, we consider in detail a specific single user system where source and relay adopt a block distributed Alamouti strategy, for transmission over frequency selective channels. We show the performance achieved over simulated as well as real data. Although DSTC follows the main ideas of conventional space-time coding (STC) techniques, there are aspects that clearly differentiate DSTC from STC. The main differences are related to the fact that in DSTC the cooperating antennas are not co-located. This implies that the signals received by the destination from source and relays might arrive out of synchronization and without the right power balance between them. We analyze these aspects in Section III-C, where we consider possible ways to distribute the power

between source and relays optimally, in order to minimize the average BER, and in Section III-F, where we consider the synchronization problem.

The performance of a cooperative network improves as the density of the relay nodes increases. However, taking into account both technical as well as economic factors, this implies that a cooperative strategy is appealing only if the cost of the relay nodes is extremely small. One possibility is to use as relays, in cellular networks, portable phones that are in standby, whose owners have previously agreed on their availability to act as relays, maybe against appropriate incentives. The other possibility consists in deploying extremely simple relays, such as for example non-regenerative, or amplify-and-forward (A&F), relays that amplify and forward the received messages. Such relays need only the radio-frequency section (antenna and amplifier) and are then much more economical than any other transceiver. To assess the performance of such relays, in Section IV we compare the performance of regenerative, i.e. decode-and-forward (D&F), relays and non-regenerative relays. In Section V we compare alternative DSTC strategies for a multi-user system. Finally, in Section VI, we derive the outage probability of a relay scheme composed of the cascade of a broadcasting channel followed by a virtual MIMO channel.

I. ON THE CONNECTIVITY OF COOPERATIVE VS. NON-COOPERATIVE WIRELESS COMMUNICATION NETWORKS

In a seminal work, Gupta and Kumar derived the conditions for the asymptotic connectivity of a network composed of nodes uniformly distributed over a disc of unit area, as the number of nodes goes to infinity [8]. In this section, we incorporate the channel fading and we provide the conditions for the network connectivity, in case of single or multi-antenna transceivers. In particular, we derive closed form, albeit approximate, expressions for the spatial density with which the nodes must be deployed in order to insure the network connectivity with a desired probability. Finally, we show how to improve the connectivity by allowing nearby nodes to transmit in a cooperative manner, using a distributed space-time coding strategy, in order to get spatial diversity gain.

One of the fundamental issues in the design of a wireless network is the minimal transmit power that guarantees the network connectivity, i.e. the property that each node is connected to each other node. In a seminal work, Gilbert modeled the network topology as a homogeneous two-dimensional Poisson point process, with constant density λ , where two points are linked if their distance is less than a coverage radius $r(n)$ that depends, on its turn, on the transmit power as well as on the number of nodes n [9]. Starting from this simple, yet meaningful, model and applying, for the first time, basic concepts from

continuum percolation, Gilbert showed that there exists a critical value λ_c of the node density such that, for $\lambda < \lambda_c$ the network is disconnected whereas for $\lambda > \lambda_c$ there is a nonnull probability that the network contains a giant component composed of an infinite number of nodes, thus creating the possibility for long distance communications through multiple hops [9]. Of course, the existence of a component with infinite nodes does not guarantee the network connectivity, as some nodes could be isolated from that giant component. The connection between continuum percolation, covering strategies and the geometry of wireless networks has been further investigated quite recently in [10].

In another fundamental paper, Gupta and Kumar derived the minimum (critical) power that guarantees the network connectivity with probability one [8]. More specifically, Gupta and Kumar proved that if the network is composed of a set of n nodes randomly distributed over a disc of unit area and each node transmits with a power that allows the coverage of a circle of radius $r(n)$ that scales with the number of nodes n as follows

$$r = \sqrt{\frac{\log n + c(n)}{\pi n}}, \quad (1)$$

the network is asymptotically connected with probability one if and only if $c(n)$ tends to infinity as n goes to infinity.

In this work we assume, as in Gilbert's work, a homogeneous Poisson point process and we find the coverage radius $r_0(n)$ that guarantees that there are no isolated nodes, where the connection between nodes is defined in terms of out-of-service probability, with respect to a target BER, for a given channel fading model. Then, exploiting Penrose's theorem [48] on the relationship between the connectivity and the degree of a random geometric graph, we derive asymptotic results on the network connectivity. Building on these derivations, we show how the connectivity improves by using multiantenna terminals. Finally, we extend the analysis to cooperative networks where nearby nodes, i.e. nodes within the coverage of each other, transmit in a coordinated manner according to a distributed space-time coding strategy, in order to achieve transmit diversity gain.

A. Connectivity of a random geometric graph

We start reviewing some results on the connectivity of geometric random graphs, as derived by Bettstetter in [47]. We assume that the nodes are distributed according to a two dimensional (2D) Poisson point process, with constant spatial density ρ . One of the key properties of this kind of point process

is that the pdf of the distance between a point and its nearest neighbor is a Rayleigh pdf. In formulas, denoting with Ξ the random variable indicating the distance between one node and its nearest neighbor, the pdf of Ξ is

$$p_{\Xi}(\xi) = 2\pi\rho\xi e^{-\rho\pi\xi^2}, \quad (2)$$

where ρ is density of the Poisson process. Starting from (2), and denoting by $r_0(n)$ the coverage radius of each node, the probability that a node is isolated is

$$P_{\text{isolated}} = 1 - P\{\xi \leq r_0(n)\} = e^{-\pi\rho r_0^2(n)}. \quad (3)$$

The probability that there are no isolated nodes or that, equivalently, the degree of the graph is strictly greater than zero, is, approximately [47]

$$p_{\text{con}} \simeq (1 - e^{-\pi\rho r_0^2(n)})^n. \quad (4)$$

This expression is approximated as it implicitly assumes that the events for which the nodes are not isolated are statistically independent of each other, which is not true, in general. Nevertheless, the validity of this approximation was tested in [47] and we will also test it through simulation results later on. Indeed, the validity of the approximation depends on the product $\rho r_0^2(n)$. If $\rho r_0^2(n) \ll 1$, the approximation is clearly not valid at all. Conversely, if $\rho r_0^2(n) \gg 1$, the approximation is more and more valid. On the other hand, since we are interested in the event that the network is connected with high probability, i.e. p_{con} is close to one, this implies that we are interested in the case where the product $\rho r_0^2(n)$ is high. This means that we can use the above approximation in cases of practical interest. Within the validity of the approximation leading to (4), inverting (4), the coverage radius r_0 that ensures that the degree of the network is greater than zero is:

$$r_0(n) = \sqrt{\frac{-\log(1 - p_{\text{con}}^{1/n})}{\pi\rho}}. \quad (5)$$

Of course, this radius does not guarantee the network connectivity, as the network could be composed of isolated clusters, with no isolated nodes. In general, in fact, the radius that guarantees the global connectivity is greater than the radius that simply guarantees that the degree of the network is strictly greater than zero. Nevertheless, Penrose proved that there is a basic relationship between connectivity and degree of a geometric graph [48]. In particular, Penrose proved that, denoting with $r(\kappa \geq k)$ the minimum distance r_0 such that a random graph is k -connected and with $r(\delta \geq k)$ the minimum distance such that the graph has minimum degree k , then [48]

$$\lim_{n \rightarrow \infty} \Pr\{r(\kappa \geq k) = r(\delta \geq k)\} = 1, \quad \forall k. \quad (6)$$

This means that, asymptotically as n tends to infinity, the coverage radius that insures a degree k tends to coincide with the radius that yields connectivity k . Hence, the equivalence (6) guarantees that, asymptotically, as n tends to infinity, the radius $r_0(n)$ in (5) tends to coincide with the radius that guarantees also the connectivity. Hence, the value $r_0(n)$ in (5) denotes, approximately, the minimum coverage that each node has to provide in order to guarantee the connectivity of the whole graph, with a given probability.

At a first glance, it might appear that the coverage radius $r_0(n)$ in (5) contradicts Gupta and Kumar

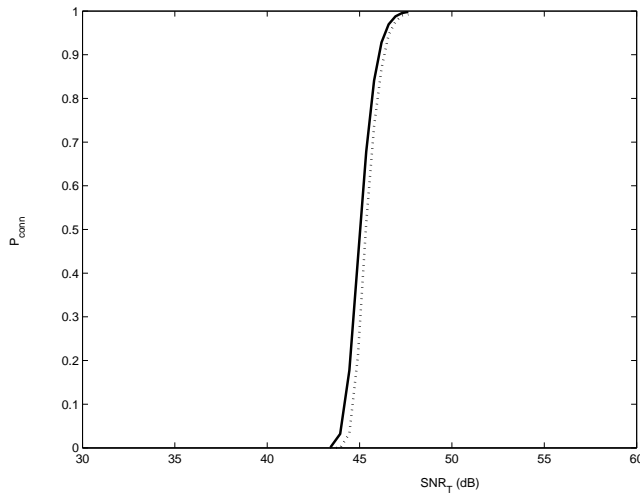


Fig. 1. Probability of connectivity vs. SNR_T reported at the transmit side (p_T/N_0) for a network composed of $n = 1000$ nodes uniformly distributed over a square of $200 \times 200m^2$.

result, recalled in (1). On the contrary, we show next that (5) and (1) are indeed in good agreement. In fact, if we rewrite the connectivity probability $p_{con}(n)$ as $p_{con}(n) = 1 - \epsilon(n)$, with $\epsilon(n) \ll 1$, we may use the first order Taylor series expansion of $p_{con}(n)^{1/n}$ as $p_{con}(n)^{1/n} \approx 1 - \epsilon(n)/n$. As a consequence, (5) becomes, approximately,

$$r_0(n) \approx \sqrt{\frac{\log n - \log \epsilon(n)}{\pi \rho}}. \quad (7)$$

Since in Gupta and Kumar the node density is $\rho = n$, inserting this value in (7), we can verify that (1) is in perfect agreement with (5) if we set $c(n) = -\log(\epsilon(n))$. In fact, requiring asymptotic connectivity with probability one implies that $\lim_{n \rightarrow \infty} \epsilon(n) = 0$ and this corresponds to the condition $\lim_{n \rightarrow \infty} c(n) = \infty$ found in [8]. Interestingly, the equivalence between these two different derivations provides also a meaning to

the term $c(n)$ appearing in [8].

A test of validity of the approximations leading to (4) is reported in Fig. 1, that shows p_{con} as a function of the SNR (referred to the transmit side), defined as $\text{SNR}_T := p_T/N_0$, as given in (4) (solid line), and the probability that the network is connected (dashed line), estimated over 200 independent realizations of random geometric graphs composed of 1000 points distributed over a toroidal surface, to avoid border effects. We can see a very good agreement between theory and simulation. The slight difference is due to the fact that the independence assumption is not exactly valid and that (6) is valid only for n going to infinity. It is interesting to notice, from Figure 1, the rapid change from probability zero to probability one. This is indeed a characteristic of random geometric graphs, that is reminiscent of phase transitions in chemistry.

If we wish to increase the fault tolerance of the graph, we need to increase the connectivity order. It was shown in [47] that the probability that a graph is k -connected is approximately equal to the probability that the minimum degree of the graph is at least k ; that is

$$\begin{aligned} \Pr_k &:= \Pr\{G \text{ is } k\text{-connected}\} \simeq \Pr\{d_{\min} \geq k\} \\ &= \left[1 - \sum_{i=0}^{k-1} \frac{(\rho\pi r_0^2)^i}{i!} e^{-\rho\pi r_0^2} \right]^n. \end{aligned} \quad (8)$$

This expression does not admit an inverse in closed form, but it is certainly invertible as it is a monotonic increasing function of r_0 . The value of r_0 providing the desired value \mathcal{P}_k , to be found numerically, guarantees the k -connectivity, within the limits of approximations in (8).

B. Connectivity of a Wireless Network

In a wireless network, besides the position of the radio nodes, there is one more source of randomness: the fading of the radio links. The connectivity of a wireless network is then, in general, much more difficult to study than the connectivity of a random graph. An interesting recent approach is proposed in [13] (see also the references therein). In this section, we propose an alternative definition of connectivity of a wireless network. In case of fading, it is in fact necessary to start with the definition of connectivity. We introduce the out-of-service probability P_{out} , defined as the probability that the bit error rate (BER) exceeds a target BER, let us say P_0 , and we say that two nodes are linked to each other if the out-of-service probability on their link does not exceed the prescribed value P_{out} . This is equivalent to say that the BER on the link may exceed the target BER for no more than a percentage P_{out} of time.

In the following sections, we show how to choose the coverage radius in order to accommodate for such a system requirement. To simplify the theoretical analysis, we assume that the channels between different pairs of nodes are independent Rayleigh flat-fading channels, with variance σ_h^2 , and that all links are interference-free. This means that there is an implicit MAC protocol that guarantees the users' separability.

C. Connectivity of a SISO Flat-Fading Network

Using QAM constellations, the bit error rate on a SISO flat fading channel is

$$P_e = c_M Q \left(\sqrt{g_M \frac{\mathcal{E}_b}{N_0} |h|^2} \right) \leq c_M e^{-g_M \mathcal{E}_b |h|^2 / N_0}. \quad (9)$$

where \mathcal{E}_b is the energy per bit, N_0 is the noise variance, h is the flat-fading coefficient, and c_M and g_M are two coefficients that depend on the order M of the QAM constellation as follows [32]

$$\begin{aligned} c_M &= 4 \frac{\sqrt{M} - 1}{\sqrt{M} \cdot \log_2 M}, \\ g_M &= \frac{3}{M - 1} \log_2 M. \end{aligned} \quad (10)$$

We assume that the channels are Rayleigh fading, so that $|h|^2$ is an exponential random variable with expected value $\sigma_h^2 = 1/r^\alpha$, where r is the link length and the exponent α depends on the environment where the propagation takes place. Typically, α is between two and six. Exploiting the upper bound in (9), we can upper-bound the out-of-service probability as

$$P_{\text{out}} = \Pr\{P_e > P_0\} \leq \Pr\{c_M e^{-g_M \mathcal{E}_b |h|^2 / N_0} > P_0\}. \quad (11)$$

Hence P_{out} can be upper-bounded as

$$P_{\text{out}} \leq 1 - e^{-N_0 \log(c_M/P_0)/(g_M \mathcal{E}_b \sigma_h^2)}. \quad (12)$$

We say that a link is reliable, and it is then established, if the out-of-service event occurs with a probability smaller than a given value. Setting $\sigma_h^2 = 1/r^\alpha$ in (12) and inverting (12), we find the coverage radius

$$r_{\text{cov}} = \left[-\frac{g_M \mathcal{E}_b \log(1 - P_{\text{out}})}{N_0 \log(c_M/P_0)} \right]^{1/\alpha}. \quad (13)$$

Since P_{out} is typically small, we can use the approximation $\log(1 - P_{\text{out}}) \approx -P_{\text{out}}$ to rewrite (13) as

$$r_{\text{cov}} \simeq \left[\frac{g_M \mathcal{E}_b P_{\text{out}}}{N_0 \log(c_M/P_0)} \right]^{1/\alpha}. \quad (14)$$

Equating (14) to (5), we get the relationship between the node density and the transmitted power necessary to insure the network connectivity, for a given number of nodes n . For example, the minimum SNR that guarantees the network connectivity, with probability p_{con} , for a given node density ρ , is:

$$\frac{\mathcal{E}_b}{N_0} \Big|_{min} \simeq \frac{\log(c_M/P_0)}{g_M P_{out}} \left(\frac{-\log(1-p_{con}^{1/n})}{\pi\rho} \right)^{\alpha/2}. \quad (15)$$

As expected, we see that to achieve a desired probability of connectivity, we can decrease the transmitted energy if we increase the node density ρ^1 . At the same time, the transmitted energy must increase when α increases. In a sensor network scenario, where it is important to foresee, a priori, the density with which the nodes should be deployed, in a given area, in order to guarantee a certain probability of connectivity, (15) can be rewritten by making explicit the minimum node density ρ that guarantees the connectivity, for a given set of sensors having a specified transmitted power

$$\rho_{min} = \frac{-\log(1-p_{con}^{1/n})}{\pi} \left(\frac{N_0 \log(c_M/P_0)}{\mathcal{E}_b g_M P_{out}} \right)^{2/\alpha}. \quad (16)$$

D. Connectivity of a MIMO Flat-Fading Network

We show now how the connectivity improves if the radio nodes have multiple antennas. In such a case, the network may benefit from the diversity gain. To make a fair comparison with the single antenna case seen before, denoting with n_T the number of transmit/receive antennas, we set the power transmitted by each antenna equal to p_T/n_T , where p_T is the overall transmit power.

Using an $n_T \times n_T$ MIMO system, using a space-time coding technique capable of achieving full diversity, the error probability is

$$P_e = c_M Q \left(\sqrt{g_M \frac{\mathcal{E}_b}{N_0 n_T} \sum_{i=1}^{n_T^2} |h_i|^2} \right) \leq c_M e^{-g_M \mathcal{E}_b z / N_0 n_T}, \quad (17)$$

having introduced, in the last approximation, the random variable $z := \sum_{i=1}^{n_T^2} |h_i|^2$. The out-of-service probability can then be upper bounded as follows

$$P_{out} = D_Z \left(\frac{N_0 n_T \log(c_M/P_0)}{g_M \mathcal{E}_b} \right),$$

¹We must keep in mind, however, that this result has been obtained by assuming lack of interference.

where $D_Z(z)$ is the cumulative distribution function (CDF) of z . If the channels are Rayleigh fading, independent, and all with the same variance σ_h^2 , the CDF of z is

$$D_Z(z) = 1 - e^{-z/\sigma_h^2} \sum_{k=0}^{n_T-1} \left(\frac{z}{\sigma_h^2} \right)^k \frac{1}{k!}. \quad (18)$$

For small values of z , more specifically for $z \ll \sigma_h^2$, $D_Z(z)$ can be approximated as

$$D_Z(z) \approx \left(\frac{z}{\sigma_h^2} \right)^{n_T^2} \frac{1}{n_T^2!}. \quad (19)$$

For the sake of finding closed form, albeit approximated, expressions, it is useful to introduce the normalized random variable $x = z/\sigma_h^2$, whose CDF is

$$D_X(x) = 1 - e^{-x} \sum_{k=0}^{n_T^2-1} x^k \frac{1}{k!} \approx \frac{x^{n_T^2}}{n_T^2!}. \quad (20)$$

Repeating the same kind of derivations as in the SISO case, the out-of-service probability for the MIMO case can be written as

$$P_{\text{out}} \leq D_X \left(\frac{N_0 n_T \log(c_M/P_0)}{g_M \mathcal{E}_b \sigma_h^2} \right). \quad (21)$$

From (21), setting $\sigma_h^2 = 1/r\alpha$, we can derive the coverage of each node²

$$r_{\text{cov}} = \left[\frac{g_M \mathcal{E}_b}{N_0 n_T \log(c_M/P_0)} D_X^{-1}(P_{\text{out}}) \right]^{1/\alpha}. \quad (22)$$

To derive an approximate closed form expression for r_{cov} , since we are interested in small values of the out-of-service probability, we can use the approximation (20) to invert $D_X(x)$. The result is

$$r_{\text{cov}} \simeq \left[\frac{g_M \mathcal{E}_b}{N_0 n_T \log(c_M/P_0)} (n_T^2! P_{\text{out}})^{1/n_T^2} \right]^{1/\alpha}. \quad (23)$$

Equating (22) to (5), we get the minimum transmit power guaranteeing the connectivity of a MIMO network

$$\frac{\mathcal{E}_b}{N_0} = \frac{n_T \log(c_M/P_0)}{g_M (n_T^2! P_{\text{out}})^{1/n_T^2}} \left[\frac{-\log(1 - p_{\text{con}}^{1/n})}{\pi \rho} \right]^{\alpha/2}. \quad (24)$$

As a numerical example, in Figure 2 we show the density ρ , as a function of the transmitted energy per bit, normalized to the noise power, for different numbers of antennas per terminal. For a fair comparison, all curves refer to the same overall transmitted power. The constellation is QPSK. The overall number of transmit/receive antennas is also the same in all cases. More specifically, we used the following combinations: $n = 100$ and $n_T = 1$ (dotted line), $n = 50$ and $n_T = 2$ (dashed line), and $n = 25$ and

² $D_X^{-1}(x)$ denotes the inverse of $D_X(x)$ and it certainly exists because in this case $D_X(x)$ is strictly monotone.

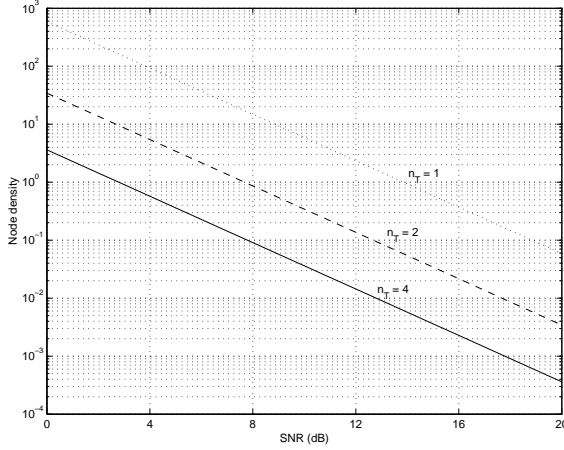


Fig. 2. Node density (number of nodes per area unit) versus \mathcal{E}_b/N_0 , for different number of antennas per terminal.

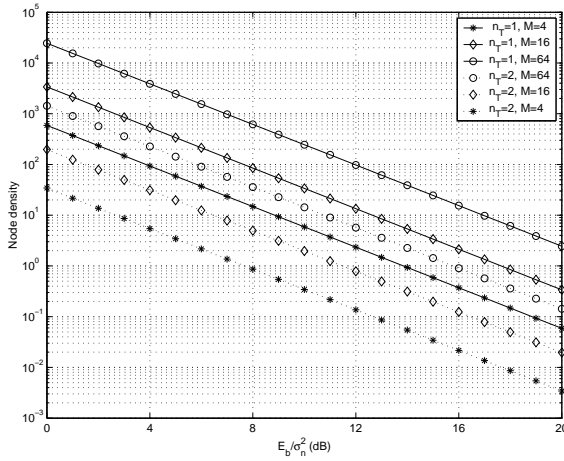


Fig. 3. Node density (number of nodes per area unit) versus \mathcal{E}_b/N_0 , for different number of antennas per terminal ($n_T = 1$ or 2) and different transmission rates ($M = 4, 16, 64$).

$n_T = 4$ (solid line). The connectivity is insured with probability $p_{\text{con}} = 0.99$ and the out-of-service event refers to a target BER of 10^{-3} and it is required to occur with a maximum time percentage of $P_{\text{out}} = 10^{-2}$. We can see, from Figure 2, the advantage of diversity that makes possible a considerable decrease of the nodes density. Clearly, terminals with multiple antennas provide a larger coverage than single antenna terminals, but at the cost of increased complexity.

The connectivity is also a function of the bit rate. As an example, in Figure 3 we show the minimum SNR required for connectivity, assuming an efficiency of 2, 4, and 6 bits/sec/Hz, achieved using 4, 16,

or 64-QAM constellations. As expected, an increase of rate requires an increase of node density, for a given power budget. Hence, the bit rate may result as a compromise between the number of antennas, node density, energy per node, and complexity.

E. Cooperative Communications

The next question is “What can we do to improve the connectivity if we have only single antenna transceivers?”. We can resort to cooperation among nearby terminals. The idea is pictorially sketched in Figure 4, where we see three nodes, A , B , and C . In the absence of any cooperation, each node covers a circle of radius r_0 given by (13). For example, in Figure 4, A and B are connected, but C is isolated. However, if nodes A and B cooperate, they can give rise to a *virtual* transmit array capable of covering

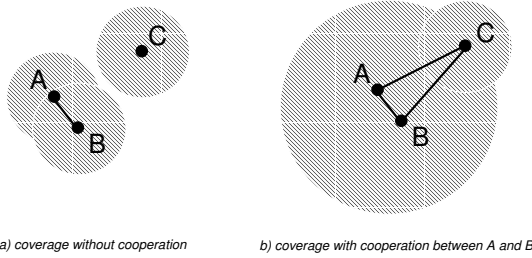


Fig. 4. Coverage in cooperating networks.

an area larger than that covered with a single antenna [22] (see also [50] and the references therein). The idea is represented, pictorially, in Figure 4 (b), where the bigger circle is the area covered by a system located in the center of gravity of the nodes A and B , with a bigger radius resulting from the use of a MISO system with two transmit and one receive antenna. Proceeding as in the previous section, denoting with n_{relay} the number of cooperating (relay) nodes, we have the potential of diversity gain $n_{\text{relay}} + 1$ (the relays plus the source itself). The existence of the bigger circle is a result of the cooperation between A and B . Thanks to cooperation, a disconnected network may become connected, as shown in the example of Figure 4 (b), using the same overall transmit power.

Let us now quantify how much is the coverage increase, due to cooperation, and how this affects the connectivity. If we have n_{relay} relays cooperating with a source and a destination with one receive antenna, the (maximum) diversity gain is $n_T := n_{\text{relay}} + 1$. Repeating derivations similar to the ones described in the previous section, with the only exception that now we only have transmit diversity, but

no receive diversity because each receiver has a single antenna, the coverage radius in case of cooperation is

$$r_{\text{coop}} \simeq \left[\frac{g_M \mathcal{E}_b}{N_0 n_T \log(c_M/P_0)} (n_T! P_{\text{out}})^{\frac{1}{n_T}} \right]^{\frac{1}{\alpha}} = \beta r_{\text{cov}}, \quad (25)$$

where r_{cov} is given by (14) and

$$\beta := \left[\frac{(n_T!)^{\frac{1}{n_T}}}{n_T P_{\text{out}}^{(n_T-1)/n_T}} \right]^{\frac{1}{\alpha}}. \quad (26)$$

Therefore, the coverage increases by a factor β that depends on the number of cooperating nodes and on the desired out-of-service probability.

The effect of the coverage increase on the network connectivity is illustrated in Figure 5, where we report the connection probabilities obtained without cooperation (dashed line) and with cooperation (solid line). In case of cooperation, we considered only the case of no more than two cooperating terminals. The probabilities shown in Figure 5 have been estimated over a set of 200 independent network realizations. As a comparison term, we report in Figure 5 the connection probability of a non-cooperative network, but having a coverage radius βr_{cov} (dotted line). We can see that cooperation between pairs of radio

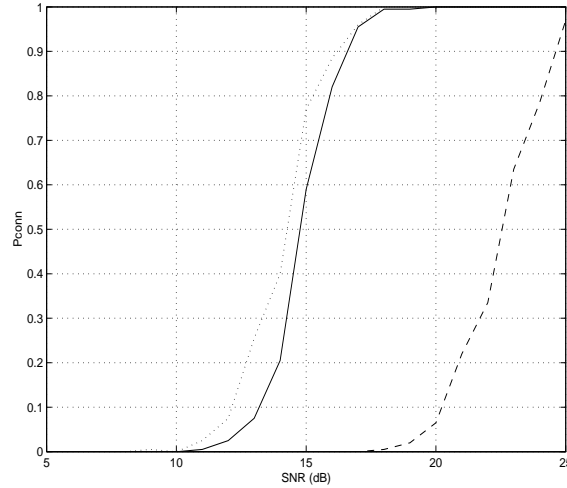


Fig. 5. Connection probabilities versus SNR (dB): without cooperation (dashed line), with cooperation (solid line), and without cooperation, but using βr_{cov} instead of r_{cov} (dotted line).

nodes is sufficient to yield an SNR gain of approximately seven dB. Interestingly, the curve obtained without cooperation, but with a coverage radius βr_{cov} has approximately the same connectivity as the cooperative case, where the coverage of each node is r_{cov} . Recalling, from (25), that the transmitted

power is proportional to r^2 , if r is the coverage, we infer that cooperation among pairs of terminals yields an improvement in terms of transmitted power approximately equal to β^2 , when $n_T = 2$.

In conclusion, the approximate expressions derived in this paper have been shown to fit quite well the behavior of wireless networks having a random topology, modeled as a 2D Poisson point process, in terms of connectivity. The formulas, albeit approximate, help to predict the gain achievable by using multiantenna terminals, either real or virtual, i.e. through cooperative communications. We have derived expressions for the density with which the network nodes should be deployed in order to guarantee the network connectivity with a desired probability. In this paper, we have only shown results concerning Rayleigh fading channels. We have extended the analysis to Nakagami- m -fading channels and we showed that the advantage decreases as the index m increases, i.e. as the channel tends to be less and less random.

F. Cooperation gain

The probability that k nodes fall within any given circle of radius r_0 is then

$$p_R(k) = \frac{(\rho\pi r_0^2)^k}{k!} e^{-\rho\pi r_0^2}. \quad (27)$$

For any given transmit power, (27) gives the probability of finding k relays. The coverage radius r_0 , on its turn, depends on the energy \mathcal{E}_b , as well as on the transmission rate (throughout the two coefficients c_M and g_M). Clearly, increasing \mathcal{E}_b , the coverage increases, but more energy is wasted only to send information towards the relays instead of the final intended destination. There is in general an optimal energy distribution between the two phases where the source sends data to the relay and when source and relays transmit together towards the destination. Let us denote by \mathcal{E}_T the total energy per bit for all cooperating nodes. Introducing the real coefficient β , with $0 \leq \beta \leq 1$, we indicate with $\beta\mathcal{E}_T$ the portion of the total energy dedicated to send information from the set of cooperating nodes to the destination and with $(1 - \beta)\mathcal{E}_T$ the energy spent by the source to send data to the relays.

If k is the number of relays that receive the data from the source with the prescribed reliability, the k relays plus the source can then transmit together towards the destination as if they were the transmit antennas of a single user³. Denoting with h_i the channel coefficients from source and relays towards the destination, using a full-diversity space-time coding scheme, such as, e.g., orthogonal coding, the error

³Since a node is chosen as a relay only if its BER is below a given threshold, with a given outage probability, we assume here that the errors at the relay nodes are negligible.

probability at the receiver is⁴

$$P_e(k+1; \mathbf{h}) = c Q \left(\sqrt{g \frac{\beta \mathcal{E}_T}{\sigma_n^2 (k+1)} \sum_{i=1}^{k+1} |h_i|^2} \right). \quad (28)$$

Assuming that the channels are statistically independent, the expected value of $P_e(k+1) := E_{\mathbf{h}}\{P_e(k+1; \mathbf{h})\}$ is [33]

$$P_e(k+1) = \frac{4\sqrt{M}-1}{\sqrt{M} \log_2(M)} \left(\frac{1-\mu}{2} \right)^{(k+1)n_R} \cdot \sum_{m=0}^k \binom{k+m}{m} \left(\frac{1+\mu}{2} \right)^m, \quad (29)$$

where

$$\mu := \sqrt{\frac{3\beta \mathcal{E}_T \log_2(M) \sigma_h^2}{3\beta \mathcal{E}_T \log_2(M) \sigma_h^2 + 2(M-1)(k+1)\sigma_n^2}}. \quad (30)$$

The final average error probability at the destination, in case of cooperation, is then

$$\overline{P}_e = \sum_{k=0}^{\infty} p_{r_0}(k) P_e(k+1), \quad (31)$$

where $p_{r_0}(k)$ is given by (27), with r_0 given by (13) setting $\mathcal{E}_b = (1-\beta)\mathcal{E}_T$, whereas $P_e(k+1)$ is given by (29). An example of average BER is reported in Fig. 6, for a network of nodes with different node

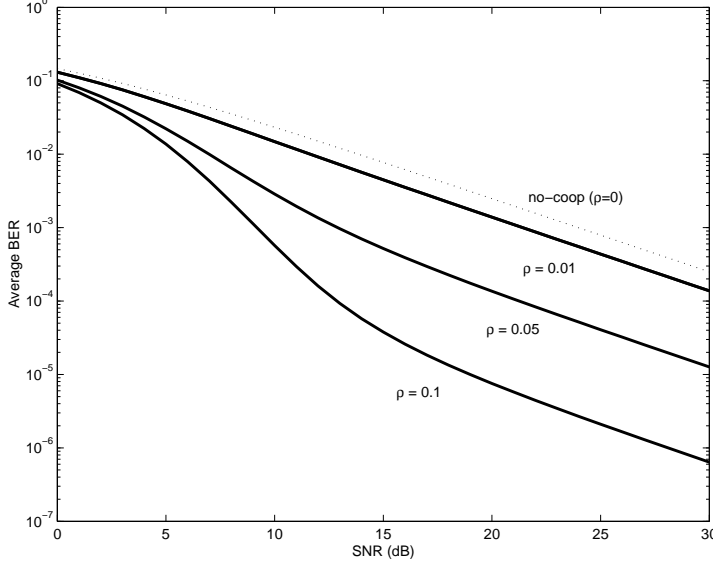


Fig. 6. Average BER at the final destination in a cooperating network for different values of node density.

⁴In case of coordinated transmission from $k+1$ nodes, we normalize the transmit power of each node by $k+1$, so that the overall radiated power is independent of k .

densities. We can clearly see the advantage of using cooperation with respect to the non-cooperative case and how the gain increases as the node density increases. At high SNR, the dominant term in (31) is the term with $k = 0$, as it corresponds to the slowest decay rate of the average bit error rate. The term $P_e(1)$ goes like $1/SNR$, at high SNR. Hence, in a random network there is no real diversity gain. Nevertheless, since $P_e(1)$ is multiplied by $p_R(0)$, there still is a coding gain equal to $1/p_R(0)$, i.e.

$$G_c = e^{\pi\rho r_0^2}. \quad (32)$$

Hence, cooperation introduces diversity, in the sense of the existence of multiple paths for the transmitted data, but unlike conventional systems, this results in a coding gain, not in a diversity gain. The coding gain is always greater than one and it grows exponentially with the increase of the relay nodes density. To obtain a higher G_c , for a given ρ , it is necessary to increase the coverage radius r_0 . This requires that more energy is used in the first phase, when S sends data to the relays. If there is a constraint on the total energy \mathcal{E}_T , it is interesting to see what is the optimal power distribution between the two transmission phases, acting on β .

As an example, in Fig. 7 we show the average BER, for a given SNR at the destination, as a function of β . We can see that, depending on the final SNR, there is an optimal β .

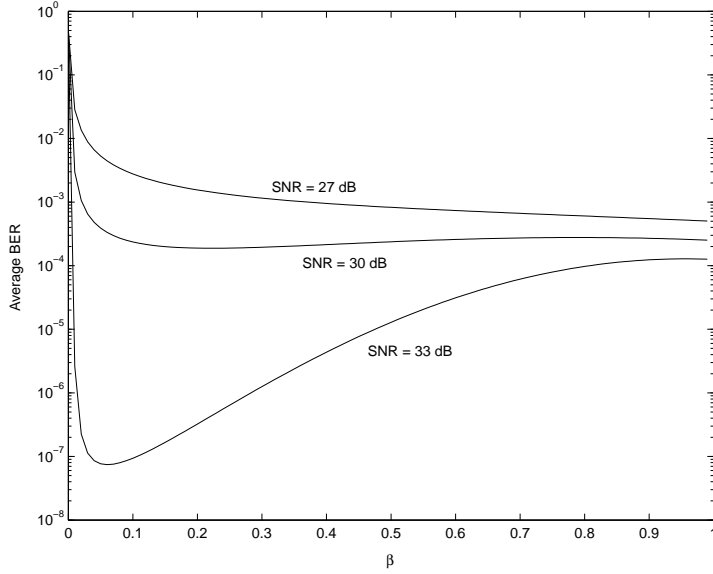


Fig. 7. Average BER as a function of β , for different SNR values.

II. DISTRIBUTED SPACE-TIME CODING

The choice of the most appropriate space-time coding technique to be used in a relay network depends on several factors. As with conventional space-time coding, the choice depends on the desired trade-off between rate, diversity and receiver complexity. The number n_R of real receive antennas plays a fundamental role. If $n_R = 1$, the cooperation induces a virtual multi-input/single output (MISO) communication, introducing diversity into the system, but not a rate gain. Conversely, if $n_R > 1$, we can think of schemes capable of both diversity and rate gains, exploiting the resulting virtual MIMO structure. Basically, one could choose among the following classes of STC techniques: i) Orthogonal STC (OSTC) [7], as a strategy that maximizes the diversity gain and it minimizes the receiver complexity; ii) full-rate/full diversity⁵ codes (FRFD) [34], [35], as codes that yield maximum diversity gain and transmission rate, but with high receiver complexity; iii) V-BLAST codes [37], as a technique that maximizes the rate, sacrificing the diversity gain, but with limited receiver complexity. Alternatively, one could use the trace-orthogonal design [38] as a flexible way to trade complexity, bit rate and bit error rate. It is worth noticing that the optimal trade-off among these alternative strategies, in the distributed case does not coincide, necessarily, with the trade-off achievable with conventional space-time coding.

The first evident difference between conventional STC and DSTC is the presence of the time slot necessary for the exchange of data between source and relays. This induces an inevitable rate loss. To reduce this loss, it is necessary to allow for the re-use of the same time slot by more than one set of source-relay pairs. In Fig. 8, we show, as an example, three sources (circles) and some potential relays (dots). If the relays are associated to the nearest sources⁶ and the sources are sufficiently far apart, we can assign the same time slot for the exchange of information between each source and its own relay. Clearly, this does not prevent the interference between different source/relay pairs. In general, the relay discovery phase should follow a strategy that gives rise to many spatially separated micro-cells, as in Fig. 8, where each source acts as a local base station broadcasting to its relays, who may get interference from other micro-cells (sources). The need to limit the coverage of each source, in its relay discovery phase, is also useful because: i) less power is wasted in the source-relay link; ii) there are less synchronization problems in

⁵The term full rate here is used in the same sense as [34], [35] and it means that a transmitter with n_T antennas transmits n_T^2 symbols in n_T time slots. This does not imply anything about the final BER and it has then to be distinguished by the information rate concept used in [36].

⁶We will comment later on the meaning of distance between source and relay, as it has to take into account also the channel fading.

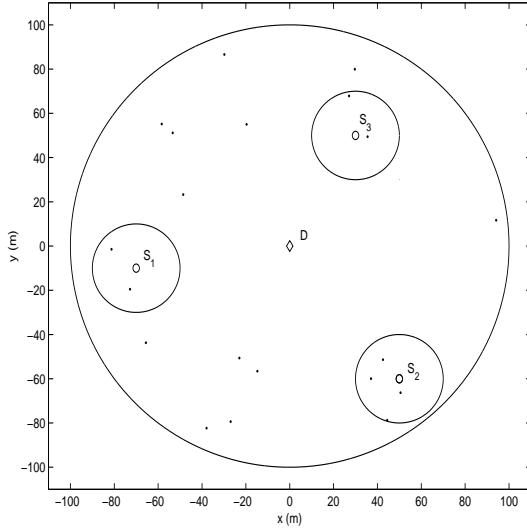


Fig. 8. Geometry of cooperative network with three source nodes (circles), potential relays (dots) and one destination (D).

the final link towards the destination; iii) there is less interference between different source/relay sets.

We now compute the rate loss for different cooperation structures, assuming that there are N simultaneous source/relays pairs sharing the same time slot. We denote with T_{S2R} and T_{SR2D} the duration of the S2R and SR2D time slots. T_s is the symbol duration in all slots. For a given bit rate, the durations depend on the constellation order used in the different slots. We denote with Q and M the constellation orders used in the S2R and in the SR2D slots, respectively. We consider a frame containing both S2R and the N SR2D links has then a duration $T_F = T_{\text{S2R}} + NT_{\text{SR2D}}$. The rate reduction factor, with respect to the non-cooperative case, in a TDMA context, is then

$$\eta = \frac{NT_{\text{SR2D}}}{T_{\text{S2R}} + NT_{\text{SR2D}}}. \quad (33)$$

Clearly, the rate loss can be reduced by decreasing T_{S2R} , i.e. by increasing Q , or by increasing N . In the first case, the relay needs a higher Signal-to-Noise-plus-Interference-Ratio (SNIR). In the second case, SNIR decreases at the relay, as there is more interference. In both cases, it is less likely to discover a relay with sufficient SNIR. Hence, the right choice has to result from a trade-off between rate and performance. We discuss now in detail the alternative DSTC strategies, corresponding to OSTC, FRFD and V-BLAST codes. In all cases, we denote with $s(n)$ the sequence of symbols sent by S during the SR2D slot, whereas $\hat{s}(n)$ indicates the estimate of $s(n)$ performed at the relay. For simplicity, we refer to a context where each source cooperates with only one relay.

A. Distributed Orthogonal STC (D-OSTC)

D-OSTC guarantees maximum receiver simplicity and full diversity and it can be implemented also when the final destination has a single antenna. D-OSTC was proposed in [22], [19], [25], where the relays are essentially error-free, and in [29], where the decoding errors at the relay are explicitly taken into account. D-OSTC transmits 2 symbols over two successive time periods, so that $T_{SR2D} = 2T_s$ and $T_{S2R} = 2 \log_2(M)T_s / \log_2(Q)$. The sequence transmitted by the source-relay pair is

$$\begin{bmatrix} s(n) & -s^*(n+1) \\ \hat{s}(n+1) & \hat{s}^*(n) \end{bmatrix}. \quad (34)$$

The first row of this matrix contains the symbols transmitted by the source, whereas the second row refers to the symbols transmitted by the relay (different columns refer to successive time instants). The overall bit rate, incorporating also the rate loss, is

$$R = \frac{2N \log_2 M}{2N + 2 \log_2 M / \log_2 Q} \text{ b/s/Hz}. \quad (35)$$

B. Distributed full rate/full diversity (D-FRFD)

If the final destination has 2 antennas, there is a virtual 2×2 MIMO, with the possibility of increasing the rate. This can be achieved, for example, using distributed-FRFD or distributed-BLAST. With D-FRFD, the pair S-R transmits 4 symbols over two consecutive time periods. The transmitted matrix is [34] or [35]:

$$\begin{bmatrix} s(n) + \varphi s(n+1) & \theta(s(n+2) + \varphi s(n+3)) \\ \theta(\hat{s}(n+2) - \varphi \hat{s}(n+3)) & \hat{s}(n) - \varphi \hat{s}(n+1) \end{bmatrix}, \quad (36)$$

where $\varphi = e^{j/2}$, $\theta = e^{j/4}$ are two rotation parameters (see, e.g. [34] or [35], for the choice of φ and θ).

The bit rate is

$$R = \frac{4N \log_2 M}{2N + 4 \log_2 M / \log_2 Q} \text{ b/s/Hz}. \quad (37)$$

C. Distributed BLAST (D-BLAST)

We consider here the version of BLAST where two independent streams of data are transmitted from the two antennas. In its distributed version, D-BLAST requires that the relay receives only half of the bits to be transmitted. This implies an advantage with respect to D-FRFD, as it allows us to reduce the duration of the S2R time slot. The price paid with respect to D-FRFD is that D-BLAST is not full diversity. The transmitted matrix in the D-BLAST case, is

$$\begin{bmatrix} s(n) & s(n+2) \\ \hat{s}(n+1) & \hat{s}(n+3) \end{bmatrix} \quad (38)$$

and the bit rate is

$$R = \frac{4N \log_2 M}{2N + 2 \log_2 M / \log_2 Q} \text{ b/s/Hz.} \quad (39)$$

Comparing the transmission rates of all the distributed schemes, for a given choice of the constellation orders Q and M , we see that D-BLAST has the highest transmission rate.

D. Relay discovery phase

This section describes a possible resource discovery phase. A source looking for potential relays starts sending a sounding signal to verify whether there are available neighbors. The sounding signal is a pseudo-noise code identifying the source. A potential relay may receive the sounding signals from more than one source. The radio nodes available to act as relays compute the signal-to-noise plus interference ratio (SNIR) for each source⁷. This step requires the node to be able to separate the signals coming from different sources. This is made possible by the use of orthogonal codes. The potential relays retransmit an acknowledgment signal back only to those sources whose SNIR exceeds a certain threshold. The source receives then the acknowledgments and the relative SNIR from all potential relays and it decides which relays to use. This phase insures that the relay, once chosen, is sufficiently reliable. Given the variability of the wireless channel, this operation has to be repeated at least once every channel coherence time. To avoid excessive complications, a node may act as a relay for no more than one source. The basic philosophy we follow to discover relays is that source and relays should be as close as possible. This is justified by the following concurring reasons: i) less power is wasted in the S2R slot; ii) there are less synchronization problems in the final SR2D slot; iii) there is less interference between different source/relay sets. In summary, this relay discovery phase creates many spatially separated micro-cells where each source acts as a local base station broadcasting to its relays, who may get interference from other micro-cells (sources).

⁷The SNIR may be evaluated for each channel realization or in average sense, considering the channel statistics such as mean and covariance. The first option provides better performance, but it requires more frequent channel estimation updates than the second option.

III. REGENERATIVE RELAYING WITH BLOCK DISTRIBUTED ORTHOGONAL SPACE-TIME CODING IN SINGLE-USER SCENARIO

In this section, we analyze in detail an example of Distributed Space-time Coding, using D-OSTC and regenerative relay [29]. We assume that the source has found its own relay⁸ and that the interference due to the other active source-relay links is negligible. We consider, thus, a two-hop relay channel, composed of a source (S), a relay (R) and a destination (D).

Differently from common STC, with DSTC, i) regenerative relays might make decision errors, so that the symbols transmitted from R could be affected by errors; ii) the links between S and D and between R and D do not have the same statistical properties, in general; iii) even if S and R are synchronous, their packets might arrive at D at different times, as S and R are not co-located. In the following, we will address all these problems specifically.

We illustrate the proposed transmission protocol by referring to a TDD scheme, but the same considerations could apply to an FDD mode. In a TDD system, each frame is subdivided in consecutive time slots: In the first slot S transmits and R receives; in the second slot, S and R transmit simultaneously. We describe the distributed space-time protocol within the following setup: (a1) all channels are FIR of (maximum) order L_h and time-invariant over at least a pair of consecutive blocks; (a2) the channel coefficients are i.i.d. complex Gaussian random variables with zero mean and variance $1/d^2$, where d is the link length; (a3) the information symbols are i.i.d. BPSK symbols that may assume the values A or $-A$ with equal probability⁹; (a4) the received data are degraded by additive white Gaussian noise (AWGN); (a5) the channels are perfectly known at the receive side and are unknown at the transmit side; (a6) the transmission scheme for all terminals is blockwise, where each block is composed of M symbols, incorporating a cyclic prefix of length L equal to the sum of the relative delay with which packets from S and R arrive at D plus the maximum channel order L_h .

We will use the following notation. We denote with h_{sd} , h_{sr} , and h_{rd} , the impulse responses between S and D , S and R , and R and D , respectively. Each block of symbols $\mathbf{s}(i)$ has size M and it is linearly encoded, so as to generate the N -size vector $\mathbf{x}_s(n) := \mathbf{F}\mathbf{s}(n)$, where \mathbf{F} is the $N \times M$ precoding matrix. A CP of length $L \geq L_h$ is inserted at the beginning of each block, to facilitate elimination of inter-block interference, synchronization, and channel equalization at the receiver. \mathbf{A}^\dagger denotes the pseudo-inverse of

⁸Thanks to the assumption that the relay nodes are not error-free, the probability of finding a relay in the discovery phase increases, with respect to the schemes that use a relay only if it is error-free.

⁹Assumption (a3) is made only for simplifying our derivations, but there is no restriction to use higher order constellations.

A ; $\Re\{x\}$ indicates the real part of x ; when applied to a vector, $\Re\{\mathbf{x}\}$ is the vector whose entries are the real part of the entries of \mathbf{x} .

D-OSTC, for frequency selective channels, works as follows. During the first time slot, S sends, consecutively, the two N -size information symbols blocks $\mathbf{s}(i)$ and $\mathbf{s}(i+1)$. The blocks are linearly encoded using the precoding matrix \mathbf{F} , so that the corresponding transmitted blocks are $\mathbf{x}_s(n) := \mathbf{F}_s \mathbf{s}(n)$, with $n = i, i+1$. Under (a6), after removing the guard interval at the receiver, the N -size vectors $\mathbf{y}_r(n)$ received from R are

$$\mathbf{y}_r(n) = \mathbf{H}_{sr} \mathbf{F}_s \mathbf{s}(n) + \mathbf{w}_r(n), \quad n = i, i+1, \quad (40)$$

where $\mathbf{w}_r(n)$ is the additive noise at the relay. Thanks to the insertion of the CP, the channel matrix \mathbf{H}_{sr} is $N \times N$ circulant Toeplitz and it is diagonalized as $\mathbf{H}_{sr} = \mathbf{W} \Lambda_{sr} \mathbf{W}^H$, where \mathbf{W} is the $N \times N$ IFFT matrix with $\{W\}_{kl} = e^{j2\pi kl/N}/\sqrt{N}$, whereas Λ_{sr} is the $N \times N$ diagonal matrix, whose entries are $\Lambda_{sr}(k, k) = \sum_{l=0}^{L_h-1} h_{sr}(l) e^{-j2\pi lk/N}$.

The relay node decodes the received vectors and provides the estimated vectors $\hat{\mathbf{s}}(i)$ and $\hat{\mathbf{s}}(i+1)$.

During the successive time-slot, S and R transmit *simultaneously*, using a block Alamouti's strategy [39]. More specifically, in the first half of the second time slot, S transmits $\mathbf{x}_s(i+2) = \alpha_1 \mathbf{F} \mathbf{s}(i)$ and R transmits $\mathbf{x}_r(i+2) = \alpha_2 \mathbf{F} \hat{\mathbf{s}}(i+1)$. In the second half, S transmits $\mathbf{x}_s(i+3) = \alpha_1 \mathbf{G} \mathbf{s}^*(i+1)$ while R transmits $\mathbf{x}_r(i+3) = -\alpha_2 \mathbf{G} \hat{\mathbf{s}}^*(i)$. To guarantee maximum spatial diversity, the two matrices \mathbf{G} and \mathbf{F} are related to each other by $\mathbf{G} = \mathbf{J} \mathbf{F}^*$, as in [39], where \mathbf{J} is a time reversal (plus a one chip cyclic shift) matrix. If N is even \mathbf{J} has all null entries except the elements of position $(1, 1)$ and $(k, N-k+2)$, with $k = 2, \dots, N$, which are equal to one. If N is odd, \mathbf{J} is the anti-diagonal matrix. The two real coefficients α_1 and α_2 are related to each other by $\alpha_1^2 + \alpha_2^2 = 1$. They are introduced in order to have a degree of freedom in the power distribution between S and R , under a given total transmit power. In Section III-C, we will show how to choose α_1 (and then α_2) in order to minimize the final average BER.

After discarding the CP and using (a1), the blocks received by D in the two consecutive time-slots $i+2$, and $i+3$ are given by

$$\begin{aligned} \mathbf{y}_d(i+2) &= \alpha_1 \mathbf{H}_{sd} \mathbf{F} \mathbf{s}(i) + \alpha_2 \mathbf{H}_{rd} \mathbf{F} \hat{\mathbf{s}}(i+1) + \mathbf{w}_d(i+2) \\ \mathbf{y}_d(i+3) &= \alpha_1 \mathbf{H}_{sd} \mathbf{G} \mathbf{s}^*(i+1) - \alpha_2 \mathbf{H}_{rd} \mathbf{G} \hat{\mathbf{s}}^*(i) + \mathbf{w}_d(i+3), \end{aligned} \quad (41)$$

where \mathbf{H}_{sd} and \mathbf{H}_{rd} refer to the channels between S and D and between R and D , respectively. Exploiting, again, the diagonalizations $\mathbf{H}_{sd} = \mathbf{W} \Lambda_{sd} \mathbf{W}^H$ and $\mathbf{H}_{rd} = \mathbf{W} \Lambda_{rd} \mathbf{W}^H$, if we pre-multiply

in (41) $\mathbf{y}_d(i+2)$ by \mathbf{W}^H and $\mathbf{y}_d^*(i+3)$ by \mathbf{W}^T , we get

$$\begin{aligned}\mathbf{W}^H \mathbf{y}_d(i+2) &= \alpha_1 \Lambda_{sd} \tilde{\mathbf{F}} \mathbf{s}(i) + \alpha_2 \Lambda_{rd} \tilde{\mathbf{F}} \hat{\mathbf{s}}(i+1) + \mathbf{W}^H \mathbf{w}_d(i+2) \\ \mathbf{W}^T \mathbf{y}_d^*(i+3) &= \alpha_1 \Lambda_{sd}^* \tilde{\mathbf{G}}^* \mathbf{s}(i+1) - \alpha_2 \Lambda_{rd}^* \tilde{\mathbf{G}}^* \hat{\mathbf{s}}(i) + \mathbf{W}^T \mathbf{w}_d^*(i+3),\end{aligned}$$

where $\tilde{\mathbf{F}} := \mathbf{W}^H \mathbf{F}$ and $\tilde{\mathbf{G}} := \mathbf{W}^H \mathbf{G}$. For the sake of simplicity, we assume that OFDM is performed at both S and R nodes, so that $N = M$, $\mathbf{F} = \mathbf{W}$ and thus $\tilde{\mathbf{F}} = \mathbf{I}_N$ and $\mathbf{G} = \mathbf{W}$. We also introduce the orthogonal matrix

$$\Lambda := \begin{pmatrix} \alpha_1 \Lambda_{sd} & \alpha_2 \Lambda_{rd} \\ -\alpha_2 \Lambda_{rd}^* & \alpha_1 \Lambda_{sd}^* \end{pmatrix} \quad (42)$$

such that $\Lambda^H \Lambda := \mathbf{I}_2 \otimes \bar{\Lambda}^2$, where $\bar{\Lambda}^2 := \alpha_1^2 |\Lambda_{sd}|^2 + \alpha_2^2 |\Lambda_{rd}|^2$, whereas \otimes denotes the Kronecker product. We introduce also the unitary matrix¹⁰ $\mathbf{Q} := \Lambda (\mathbf{I}_2 \otimes \bar{\Lambda}^{-1})$, satisfying the relationships $\mathbf{Q}^H \mathbf{Q} = \mathbf{I}_{2N}$ and $\mathbf{Q}^H \Lambda = \mathbf{I}_2 \otimes \bar{\Lambda}$. Exploiting the above equalities and multiplying the vector $\mathbf{u} := [(\mathbf{W}^H \mathbf{y}_d(i+2))^T, (\mathbf{W}^T \mathbf{y}_d^*(i+3))^T]^T$ by the matrix \mathbf{Q}^H , without compromising the decision optimality (because of the unitarity of \mathbf{Q}), we get

$$\begin{aligned}\begin{bmatrix} \mathbf{r}(i) \\ \mathbf{r}(i+1) \end{bmatrix} &:= \mathbf{Q}^H \mathbf{u} \\ &= \begin{bmatrix} |\tilde{\Lambda}_{sd}|^2 & -\tilde{\Lambda}_{sd}^* \tilde{\Lambda}_{rd} \\ \tilde{\Lambda}_{sd} \tilde{\Lambda}_{rd}^* & |\tilde{\Lambda}_{sd}|^2 \end{bmatrix} \mathbf{s} + \begin{bmatrix} |\tilde{\Lambda}_{rd}|^2 & \tilde{\Lambda}_{sd}^* \tilde{\Lambda}_{rd} \\ -\tilde{\Lambda}_{sd} \tilde{\Lambda}_{rd}^* & |\tilde{\Lambda}_{rd}|^2 \end{bmatrix} \hat{\mathbf{s}} + \bar{\mathbf{w}},\end{aligned} \quad (43)$$

where $\mathbf{s} := [\mathbf{s}(i)^T, \mathbf{s}(i+1)^T]^T$, $\hat{\mathbf{s}} := [\hat{\mathbf{s}}(i)^T, \hat{\mathbf{s}}(i+1)^T]^T$, $\tilde{\Lambda}_{sd} := \alpha_1 \Lambda_{sd} \bar{\Lambda}^{-1/2}$, $\tilde{\Lambda}_{rd} := \alpha_2 \Lambda_{rd} \bar{\Lambda}^{-1/2}$, $\bar{\mathbf{w}} := [\bar{\mathbf{w}}^T(i), \bar{\mathbf{w}}^T(i+1)]^T = \mathbf{Q}^H [\mathbf{w}^T(i+2), \mathbf{w}^H(i+3)]^T$. As expected, the previous equations reduce to the classical block Alamouti equations, see e.g. [39], the two transmit antennas use the same power, i.e., $\alpha_1 = \alpha_2$, and there are no decision errors at the relay node, i.e., $\hat{\mathbf{s}}(n) \equiv \mathbf{s}(n)$, $n = i, i+1$.

Since \mathbf{Q}^H is unitary, if \mathbf{w} is white, $\bar{\mathbf{w}}$ is also white, with covariance matrix $\mathbf{C}_w = \sigma_n^2 \mathbf{I}_{2N}$. Furthermore, since all matrices Λ appearing in (43) are diagonal, the system (43) of $2N$ equations can be decoupled into N independent systems of two equations in two unknowns, each equation referring to a single sub-carrier. More specifically, introducing the vectors $\mathbf{r}_k := [r_k(i), r_k(i+1)]^T$, $\mathbf{s}_k := [s_k(i), s_k(i+1)]^T$, $\hat{\mathbf{s}}_k := [\hat{s}_k(i), \hat{s}_k(i+1)]^T$ and $\bar{\mathbf{w}}_k := [\bar{w}_k(i), \bar{w}_k(i+1)]^T$, referring to the k -th sub-carrier, with $k = 0, \dots, N-1$ (for simplicity of notation, we drop the block index and we set $\tilde{\Lambda}_{sd} = \tilde{\Lambda}_{sd}(k, k)$ and $\tilde{\Lambda}_{rd} = \tilde{\Lambda}_{rd}(k, k)$),

¹⁰We suppose that the channels do not share common zeros on the grid $z_q = e^{j2\pi q/N}$, with q integer, so that $\bar{\Lambda}$ is invertible.

(43) is equivalent to the following systems of equations

$$\mathbf{r}_k = \begin{pmatrix} |\tilde{\Lambda}_{sd}|^2 & -\tilde{\Lambda}_{sd}^* \tilde{\Lambda}_{rd} \\ \tilde{\Lambda}_{sd} \tilde{\Lambda}_{rd}^* & |\tilde{\Lambda}_{sd}|^2 \end{pmatrix} \mathbf{s}_k + \begin{pmatrix} |\tilde{\Lambda}_{rd}|^2 & \tilde{\Lambda}_{sd}^* \tilde{\Lambda}_{rd} \\ -\tilde{\Lambda}_{sd} \tilde{\Lambda}_{rd}^* & |\tilde{\Lambda}_{rd}|^2 \end{pmatrix} \hat{\mathbf{s}}_k + \bar{\mathbf{w}}_k \quad (44)$$

Since the noise vector $\bar{\mathbf{w}}_k$ is also white with covariance matrix $\mathbf{C}_w = \sigma_n^2 \mathbf{I}_{2N}$, and there is no inter-symbol interference (ISI) between vectors \mathbf{s}_k and \mathbf{r}_k corresponding to different sub-carriers, \mathbf{r}_k represents a sufficient statistic for the decision on the transmitted symbols vector \mathbf{s}_k .

A. ML detector

We derive now the structure of the maximum likelihood (ML) detector at the final destination. Besides the previous assumptions, we assume also that D has perfect knowledge of the vector of error probabilities $p_{e1}(k)$ and $p_{e2}(k)$, $k = 0, \dots, N-1$, occurring at the relay. This requires an exchange of information between R and D . This information has to be updated with a rate depending on the channel coherence time. Later on, we will show an alternative (sub-optimum) detection scheme that does not require such a knowledge.

We denote with \mathcal{S} the set of all possible transmitted vectors \mathbf{s}_k and with $p_{e1}(k)$ and $p_{e2}(k)$ the conditional (to a given channel realization) error probabilities, at the relay node, on $s_k(1)$ and $s_k(2)$, respectively. After detection, at the node R, we have $\hat{s}_k(l) = s_k(l)$, with probability $(1 - p_{el}(k))$, or $\hat{s}_k(l) = -s_k(l)$, with probability $p_{el}(k)$, $l = 1, 2$. Since the symbols are independent, the probability density function of the received vector \mathbf{z} , conditioned to having transmitted \mathbf{s}_k , is [40]

$$\begin{aligned} f_{\mathbf{z}|\mathbf{s}_k}(\mathbf{z}|\mathbf{s}_k) = & \frac{1}{\pi^2 \sigma_n^2} [(1 - p_{e1}(k))(1 - p_{e2}(k)) \exp \{-|\mathbf{z} - \mathbf{A}_k(1, 1)\mathbf{s}_k|^2 / \sigma_n^2\} \\ & + p_{e1}(k)p_{e2}(k) \exp \{-|\mathbf{z} - \mathbf{A}_k(-1, -1)\mathbf{s}_k|^2 / \sigma_n^2\} \\ & + (1 - p_{e1}(k))p_{e2}(k) \exp \{-|\mathbf{z} - \mathbf{A}_k(1, -1)\mathbf{s}_k|^2 / \sigma_n^2\} \\ & + p_{e1}(k)(1 - p_{e2}(k)) \exp \{-|\mathbf{z} - \mathbf{A}_k(-1, 1)\mathbf{s}_k|^2 / \sigma_n^2\}], \end{aligned} \quad (45)$$

where $\mathbf{A}_k(\theta_1, \theta_2)$ is defined as follows

$$\mathbf{A}_k(\theta_1, \theta_2) = \begin{bmatrix} |\tilde{\Lambda}_{sd}|^2 + |\tilde{\Lambda}_{rd}|^2 \theta_1, & \tilde{\Lambda}_{sd}^* \tilde{\Lambda}_{rd} \theta_2 - \tilde{\Lambda}_{sd}^* \tilde{\Lambda}_{rd} \\ \tilde{\Lambda}_{sd} \tilde{\Lambda}_{rd}^* - \tilde{\Lambda}_{sd} \tilde{\Lambda}_{rd}^* \theta_1, & |\tilde{\Lambda}_{sd}|^2 + |\tilde{\Lambda}_{rd}|^2 \theta_2 \end{bmatrix}.$$

Based on (45), the ML detector is

$$\hat{s}_k = \arg \max_{\mathbf{s}_k \in \mathcal{S}} \{ f_{\mathbf{r}_k | \mathbf{s}_k}(\mathbf{r}_k | \mathbf{s}_k) \}. \quad (46)$$

Note that, thanks to the orthogonal space-time block coding strategy, the optimal detector preserves the receiver's simplicity, because, under (a1)-(a6), the ML solution performs an exhaustive search only among four possible transmitted vectors \mathbf{s}_k 's.

B. Sub-optimum detector

The ML detector described above requires the knowledge, at the destination node, of the set of error probabilities $p_{e1}(k)$ and $p_{e2}(k)$, with $k = 0, \dots, N - 1$. If this knowledge is not available, a sub-optimum scalar detector can be implemented, instead of the ML detector. More specifically, the decision on the transmitted symbol $s_k(n)$ can be simply obtained as

$$\hat{s}(n) = \text{sign} \{ \Re[\mathbf{r}(n)] \}, \quad n = i, i + 1, \quad (47)$$

where $\mathbf{r}(n)$ is given by (43). Note that, for high SNR at the relay (i.e. when R makes no decision errors), the symbol-by-symbol decision in D becomes optimal and, thus, the decoding rule (47) provides the same performance as the optimal receiver (46). When the decision errors at the relay side cannot be neglected, the sub-optimal receiver introduces a floor in the bit-error-rate (BER) curve, because the symbol-by-symbol decision (47) treats the wrong received symbols as interference. The choice between the decoding rules (46) and (47) should then result as a trade-off between performance and computational complexity, taking into account the need, for the ML detector, to make available, at the destination node, the error probabilities of the relay node. We will show a comparison between ML and sub-optimum strategies in Section III-D.

C. Power Allocation between Source and Relays

While in conventional STC, the transmit antennas typically use the same power over all the transmit antennas, with DSTC it is useful to distribute the available power between source and relay as a function of their relative position with respect to the final destination, since they are not co-located. In this section we show how to distribute a given total power optimally between source and relay. We provide first a closed form analysis in the ideal case where there are no decision errors at the relay and then we will show some performance results concerning the real case where the errors are taken into account.

1) *Error-free S2R link:* Under the assumption that there are no errors at the relay side, using the same derivations introduced in Sec. III, the optimal detector is a symbol-by-symbol detector and the signal-to-noise ratio on the k -th symbol in the n -th block is

$$SNR_k(n) = \frac{A^2}{\sigma_n^2} (\alpha |\Lambda_{sd}(k, k)|^2 + (1 - \alpha) |\Lambda_{rd}(k, k)|^2), \quad (48)$$

for $k = 1, \dots, N$ and $n = i, i + 1$. The error probability for binary antipodal constellation, conditioned to a given channel realization, is given by

$$P_{e|h}(k) = \frac{1}{2} \operatorname{erfc} \left(\sqrt{0.5 SNR_k} \right) \quad (49)$$

where SNR_k is given by (48). For each sub-carrier k , the signal-to-noise ratio SNR_k is given by the sum of two statistically independent random variables, each one distributed according to a χ^2 pdf with two degrees of freedom. Thus, using (48) and (49), the BER P_b averaged over the channel realizations is given by [33]

$$P_b = \frac{1}{2} \frac{\gamma_2}{\gamma_2 - \gamma_1} \left(1 - \sqrt{\frac{\gamma_1}{1 + \gamma_1}} \right) + \frac{1}{2} \frac{\gamma_1}{\gamma_1 - \gamma_2} \left(1 - \sqrt{\frac{\gamma_2}{1 + \gamma_2}} \right), \quad (50)$$

where

$$\gamma_1 := \frac{A^2}{\sigma_n^2} \frac{\alpha \tilde{\sigma}_h^2}{d_{sd}^\alpha}, \quad \gamma_2 := \frac{A^2}{\sigma_n^2} \frac{(1 - \alpha) \tilde{\sigma}_h^2}{d_{rd}^\alpha}, \quad \tilde{\sigma}_h^2 = \sigma_h^2 (L_h + 1).$$

From (50), we infer that, if the errors in the relay's detection are negligible, D-OSTC scheme achieves, as expected, the maximum available diversity gain, equal to two. The optimum value of α can be found by minimizing (50). Since the average BER (50) is a convex function with respect to α [40], the optimal value of the minimization admits a unique solution.

It is straightforward to show that, if D is equipped with n_R antennas, the achieved diversity gain is $2 n_R$.

2) *S2R link with errors:* When the errors at the relay side are explicitly taken into account, it is not easy to derive the performance of the optimal detector (46) in closed form. In this case, it is interesting to check the performance of the sub-optimal detector (47), to quantify the loss with respect to the more complex but optimal detector (46). In [40] a closed form expression for the BER of the sub-optimum scheme, in the presence of relay decision errors, was derived. For a given total transmitted power from S and R, we can optimize the power allocation between S and R, depending on the relative distances between S, R and D, in order to minimize the final average BER. We address this issue in the following example.

Example 1 - Optimal power allocation: We show now the behavior of the final average BER as a function of the power allocation between S and R , depending on the relative distances between S , R and D . As an example, in Fig. 9 we report the average BER vs. α , as defined in Section III-C.2, for different values of the distance d_{rd} (and thus of SNR_R) between R and D (all distances are normalized with respect to the distance d_{sd} between S and D). In Fig. 9a), we consider the ideal case where there are no errors at the relay node. The SNR_D at the final destination is fixed equal to 10 dB. We can observe that, when $d_{sd} = d_{rd} = 1$, the value of α that minimizes the average BER is $\alpha = 0.5$, i.e. the two transmitter use the same power. However, as R gets closer to D , the optimal α tends to increase, i.e. the system allocates more power to S , with respect to R . The reverse happens when d_{rd} is greater than 1. Thus, as expected, the system tends to, somehow, put S and R in the same conditions with respect to D , in order to get the maximum diversity gain.

The real case, where there are decision errors at the relay node, is reported, as an example, in Fig. 9b), where the average BER is again plotted as a function of α , but for different values of the SNR_R at the relay node. Interestingly, we can observe that, as SNR_R decreases, the system tends to allocate less power to the relay node (the optimal value of α is greater than 0.5), as the relay node becomes less and less reliable.

D. Performance

In this section, we compare alternative cooperative strategies. We assume a block length $N = 32$ and channel order $L = 6$. To make a fair comparison of the alternative transmission schemes, we enforce all systems to transmit with the same overall power. More specifically, if \mathcal{P} is the total power radiated by the non cooperative scheme, we denote by \mathcal{P}_I the power radiated by S during the first time-slot and by $\alpha\mathcal{P}_{II}$ and $(1 - \alpha)\mathcal{P}_{II}$ the power spent respectively by S and R in the second time-slot. Since the overall radiated power is always \mathcal{P} , it must be $\mathcal{P} = \mathcal{P}_I + \mathcal{P}_{II}$. The coefficient α is chosen in order to minimize the final average bit-error probability (50) (see also Example 1)¹¹. The power \mathcal{P}_I is chosen in order to achieve a required average SNR_R at the relay, defined as $SNR_R := \frac{\mathcal{P}_I}{\sigma_n^2 d_{sr}^2}$. All distances in the network are normalized with respect to the distance d_{sd} between S and D .

¹¹We use theoretical derivations, valid in the absence of errors at the relay, to simplify the strategy. One could improve upon this choice by using the BER resulting in the presence of errors at the relay.

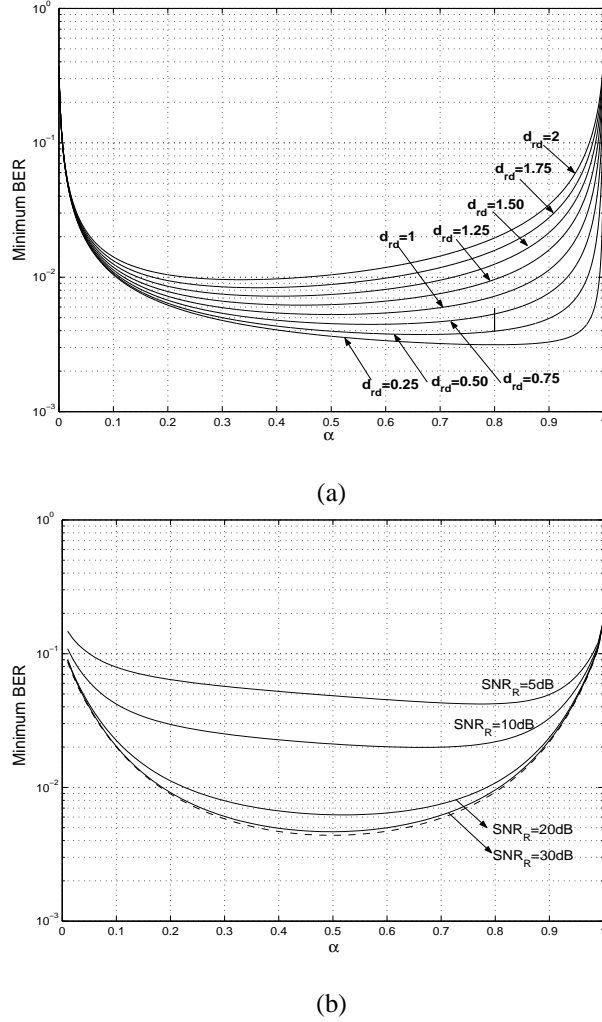


Fig. 9. Average BER vs. α ; a) no errors at R; b) including errors at R.

Example 2 - ML vs. sub-optimum detector: In Figs. 10 and 11, we compare the average BER obtained using alternative cooperative and non-cooperative schemes. The BER is averaged over 2000 independent channel realizations. All curves are plotted versus the SNR in D , defined as $SNR_D := \frac{\mathcal{P}}{\sigma_n^2 d_{sd}^2}$. This is also the SNR of the single-hop (non-cooperative) case. The variance of the noise at both R and D is unitary. In this example, we set $d_{sr} = 0.1$ and $d_{rd} = 0.9$. The results shown in Fig. 10 and 11 are achieved transmitting with a power \mathcal{P}_I yielding an average SNR_R at the relay equal to 15 dB, for all values of SNR_D reported in the abscissas. Since the noise power and SNR_R are both fixed, increasing SNR_D means that \mathcal{P}_{II} increases. In Fig. 10 and 11 we report, for the sake of comparison, the average BER obtained with the following schemes: i) the single-hop method (dotted line); ii) the ideal ML detector

for O-DSTC scheme, with no errors at the relay (dashed and dotted line); iii) the real ML detector, incorporating the decision errors at the relay (dashed line); iv) the sub-optimum scalar decoder for O-DSTC scheme, showing both the theoretical average BER (solid line) and the corresponding simulation results (circles), obtained using a Zero-Forcing detector at the relay node. In Fig. 11 we report the performance of the optimal versus sub-optimal detector, on real wideband channel measurements, kindly provided by the group of the University of Bristol led by Prof. A. Nix and M. Beach. The data are collected in an urban environment (the city of Bristol) in the band between 1920 and 1930 MHz.

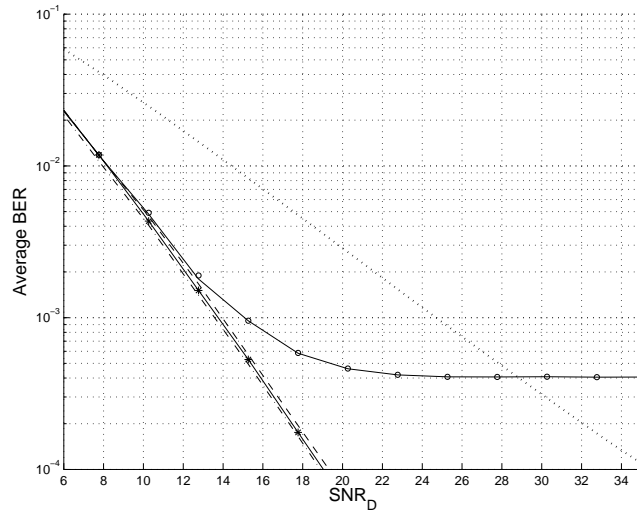


Fig. 10. Comparison between average BER vs. SNR_D (dB) achieved with different decision schemes over Rayleigh channels: Single S-D link (dotted line); ideal ML (dashed-dotted line); real ML detector (dashed line); sub-optimum receiver - theoretical results (solid line) and simulation (circles); $SNR_R = 15$ dB.

We can observe a very good agreement between our theoretical derivations for the sub-optimum detector and the corresponding simulation results. The floor on the BER of the sub-optimum receiver is due to the decision errors at the relay node. It is also interesting to notice, from Fig. 10, that the sub-optimum O-DSTC scheme exhibits performance very close to the optimal O-DSTC ML detector, at low SNR_D , i.e. before the BER floor, when the relay is relatively close to the source. This indicates that the sub-optimum detector is indeed a very good choice, under such a scenario, because it is certainly less complicated to implement than the ML detector. Most important, differently from ML, the sub-optimum scheme does not require any exchange of information between R and D , about the BER in R . The price paid for this simplicity is that the R node must have a sufficiently high SNR to guarantee that the BER of interest be above the floor. In Figs.10 we have also reported the average BER (solid line with starts) obtained

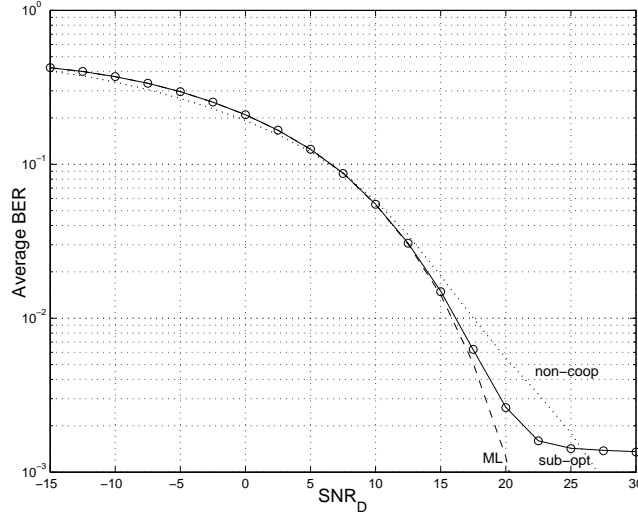


Fig. 11. Comparison between average BER vs. SNR_D (dB) achieved with different decision schemes over real channel measurements: Single S-D link (dotted line); ideal ML (dashed-dotted line); real ML detector (dashed line); sub-optimum receiver - theoretical results (solid line) and simulation (circles); $SNR_R = 15$ dB.

using a transmission strategy, for O-DSTC scheme, where instead of OFDM, in the S/R slot we used a linear precoding method that insures minimum BER at the relay, under the assumption of adopting a (suboptimal) MMSE linear decoder (solid line with stars). In such a case, we observe that, with minimum additional complexity at the relay, the performance of the suboptimal O-DSTC scheme becomes closer to the ML decoder because of the lower BER at the relay.

Finally, looking at the slopes of the average BER curves of the ML O-DSTC detector, shown in Figs.10 and 11, it is worth noticing that, in the absence of errors at the relay, the cooperative scheme achieves full spatial diversity gain, provided that the relay can be used, as we have assumed in this section. In practice, there are two reasons for the lack of full diversity gain. The first one is that, in a network where the relays are randomly spatially distributed, the probability of finding no relay is not zero. The second one is that, given a set of terminals available as relays, because of the presence of decoding errors at the relay side, all cooperative schemes exhibit an asymptotic average BER behavior proportional to $1/SNR_D$. Nevertheless, there is a considerable coding gain, which justifies the use of cooperation. Indeed, a more attentive look at the results shows that the average BER starts approaching the slope with maximum diversity, as far as the errors at the relay are negligible with respect to the errors at the destination. Then, when the errors at the relay become dominant, the final BER curve follows the $1/SNR$ behavior.

E. Choice of the Constellation Order in the Source-Relay slot

The other major critical aspect of cooperative schemes is their rate loss due to the insertion of the *S/R* time slot. As an example, if all the links would use a BPSK constellation, the rate loss factor would be 1/2. To reduce this loss factor, we can use higher order constellations in the *S/R* link, with respect to the constellations used in the other links, so that the duration of the *S/R* slot can be made smaller than the duration of the other slots. In this section, we assume BPSK transmissions over all links, except the *S/R* link, where the constellation order is allowed to increase. More specifically, using a constellation \mathcal{A} of cardinality $M = 2^{n_b}$ in the *S/R* link, the rate loss factor is $n_b/(n_b + 1)$. On the other hand, cooperation reduces the final BER and then it induces a capacity increase. To quantify the overall balance in terms of rate, we compared the maximum rate achievable by O-DSTC system with the maximum rate achievable with a non-cooperative scheme. We define as achievable rate the maximum number of bits per symbol (bps) that can be decoded with an arbitrarily low error probability, provided that sufficient error correction coding is incorporated in the system, conditioned to the assumptions (a1)-(a6)¹². We have shown in Section III that the combination of O-DSTC and OFDM makes the overall time-dispersive channel equivalent to a set of parallel non-dispersive sub-channels. The final *S2D* link, over each sub-channel, in the presence as well as in the absence of the relay link, can always be made equivalent to a binary symmetric channel (BSC) with cross-over probability depending on the specific cooperative (or non-cooperative) scheme adopted. Thus, the maximum rate $R(k|\mathbf{h})$ that can be reliably transmitted, over the k -th sub-carrier, for a given channel realization \mathbf{h} , incorporating the rate loss due to the insertion of the *S2R* slot, is

$$R(k|\mathbf{h}) = \frac{1}{1 + 1/n_b} C_{\text{BSC}}(P_{e|h}(k)) \quad \text{bps.} \quad (51)$$

where $P_{e|h}(k)$ denotes the binary error probability on the k -th sub-carrier, conditioned to the channel realizations, $C_{\text{BSC}}(p) := 1 + p \log_2(p) + (1 - p) \log_2(1 - p) := 1 - H(p)$ is the capacity of a binary symmetric channel¹³ with crossover probability p . From (51) we infer that, because of the *S2R* link, cooperative transmission induces a systematic rate loss of $n_b/(n_b + 1)$, with respect to the case of no cooperation. But, at the same time, cooperation yields a smaller error probability $P_{e|h}(k)$ and thus a higher $C_{\text{BSC}}(P_{e|h}(k))$. Then, we may expect a trade-off in the choice of n_b . This trade-off can be better understood through the following example.

¹²It is important to remark that the rate defined above is smaller than the capacity of the system, because the proposed scheme is designed to maximize the spatial diversity gain and not to maximize information rate.

¹³We can use this formula because the S-D is always BPSK, regardless of the constellation used in the *S2R* link.

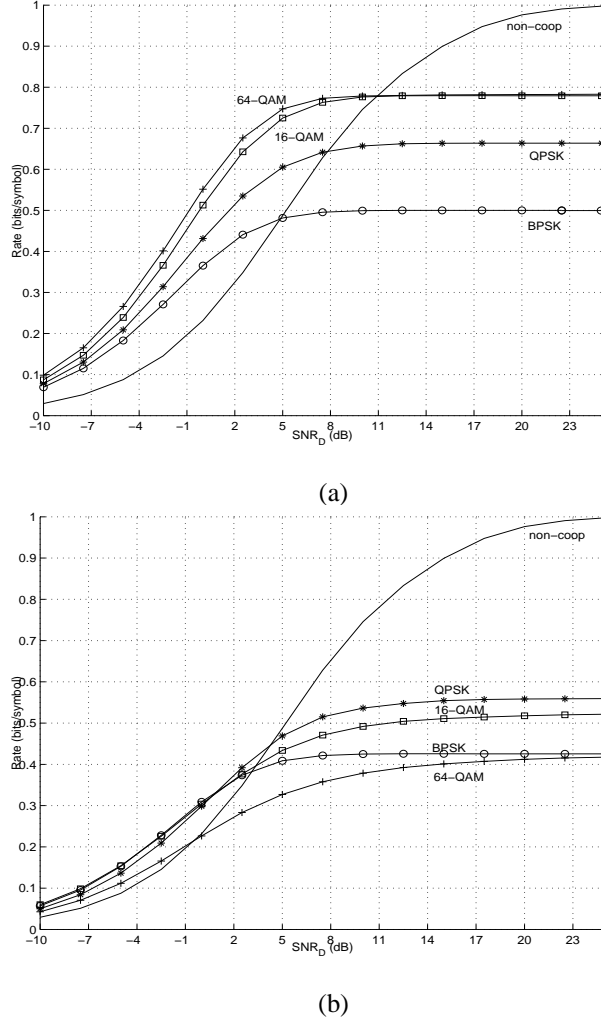


Fig. 12. Achievable rate (bps) vs. SNR (dB) - non cooperative case (solid line), cooperative case using: BPSK (circle marker), QPSK (star marker), 16-QAM (square marker), 64-QAM ('+') in the S2R link - a) $SNR_R = 15$ dB; b) $SNR_R = 3$ dB.

Example 3. Rate and diversity gain: As an example, we report in Fig.12 a) and b) the achievable rate vs. the SNR_D in D, for an SNR_R in R equal to 15 and 3 dB, respectively, for different choices of the constellation used in the S2R link, achieved with or without cooperation. To preserve the receiver simplicity, zero-forcing equalization and symbol-by-symbol detection are performed at the relay. We can see that, at high SNR_D , the non-cooperative case approaches the maximum value, equal to 1 bps, whereas the cooperative cases tend to an asymptote less than 1, depending on the constellation used in S2R slot. We observe from Fig.12 a) that, for $SNR_R = 15$ dB, increasing the constellation order from BPSK to 16-QAM in the S2R link improves the achievable rate; however passing from 16 – QAM

to $64 - QAM$ does not induce any further gain because of the higher BER at the relay. For lower values of SNR_R , i.e. $SNR_R = 3$ dB for example, there is no appreciable rate gain in increasing the constellation order because of the excessive BER at the relay. Nevertheless, it is interesting to notice that, at low/medium SNR_D at the final destination (within a range depending on SNR_R), the cooperative case can outperform the non-cooperative case also in terms of achievable rate, because the BER decrease can more than compensate the rate insertion loss due to the S2R slot.

F. Synchronization

Besides errors at the relay node, one more distinguishing feature of DSTC is that the cooperating transmit antennas are not co-located. This means that the packets arriving at the final destination from source and relays might be asynchronous. Interestingly, if the difference in arrival times τ_d is incorporated in the CP used from both S and R, D is still able to get N samples from each received block, without inter-block interference (IBI). In such a case, the different arrival time does not cause any trouble to the final receiver. In fact, let us take as a reference time the instant when the i -th block coming from R arrives at D . If the block coming from S arrives with a delay of L_d samples, the only difference with respect to the case of perfect synchronization is that the transfer function $\tilde{\Lambda}_{sd}(k)$ in (44) will be substituted by $\tilde{\Lambda}_{sd}(k)e^{-j2\pi L_d k/N}$. From (44), it is clear that such a substitution does not affect the useful term, as it only affects the interfering term. However, in the hypothesis of Rayleigh fading channel, $\tilde{\Lambda}_{sd}(k)$ is statistically indistinguishable from $\tilde{\Lambda}_{sd}(k)e^{-j2\pi L_d k/N}$. Hence, the combination of Alamouti (more generally, orthogonal STC) and OFDM is robust with respect to lack of synchronization between the time of arrival of packets from S and from R (as long as (a6) holds true). The price paid for this robustness is the increase of the CP length L , which, in its turn, reflects into a rate loss. However, this loss can be made small by choosing a blocklength N much greater than L or by selecting only relays that are relatively close to the source, so as to make the relative delay small.

IV. REGENERATIVE VS. NON-REGENERATIVE RELAYS IN SINGLE-USER SCENARIO

In non-regenerative schemes, the relay node simply amplifies and retransmits the received signal, without performing any A/D conversion on the signal. Thus, A&F can be useful to simplify the implementation of the relay, because the relay of an A&F system only needs to have an antenna and a RF amplifier.

Since no detection can be performed at the relay side in the A&F scheme, the relay can only retransmit the received signal. Thus, in order to implement the distributed version of Alamouti scheme, in the first

time-slot, S has to transmit, consecutively, the blocks $-A_s \mathbf{F} \mathbf{s}(i+1)$ and $A_s \mathbf{G} \mathbf{s}^*(i)$ ¹⁴. In the second time-slot, S transmits, consecutively, $A_s \mathbf{F} \mathbf{s}(i)$ and then $A_s \mathbf{G} \mathbf{s}^*(i+1)$ and R sends $A_r(-\mathbf{H}_{sr} \mathbf{F} \mathbf{s}(i+1) + \mathbf{v}_R(i))$ first and then $A_r(\mathbf{H}_{sr} \mathbf{G} \mathbf{s}^*(i) + \mathbf{v}_R(i+1))$. The amplitude coefficients A_s and A_r are used to impose the power available at the S and R nodes, respectively. In the A&F case, differently from the D&F case, the coefficient A_r depends also on the S2R channel as well as on the noise at the R node. Clearly, A_r changes depending on which strategy is implemented in R.

Thanks to the combination of Alamouti's coding and OFDM, the overall systems is equivalent to a series of N parallel channels. Proceeding as in Sec. III to obtain (44), the received symbol \mathbf{r}_k pertaining to the k -th sub-carrier, in the i -th and $i+1$ -th time slots is given by¹⁵

$$\mathbf{r}_k = \begin{bmatrix} g_k & 0 \\ 0 & g_k \end{bmatrix} \mathbf{s}_k + \boldsymbol{\nu}_k, \quad (52)$$

where $\mathbf{s}_k = [s_k(i), s_k(i+1)]^T$, $g_k := A_s^2 |\Lambda_{sd}(k)|^2 + A_r^2 |\Lambda_{rd}(k)|^2 |\Lambda_{sr}(k)|^2$ and $\boldsymbol{\nu}_k$ is a Gaussian vector with zero mean and diagonal covariance matrix $\mathbf{C}_\nu = \sigma_\nu^2 \mathbf{I}$, with $\sigma_\nu^2 = (A_r^2 |\Lambda_{rd}(k)|^2 \sigma_r^2 + \sigma_d^2) (A_s^2 |\Lambda_{sd}(k)|^2 + A_r^2 |\Lambda_{rd}(k)|^2 |\Lambda_{sr}(k)|^2)$.

Example 3. Comparison between A&F and D&F: In Fig. 13, we compare the average BER vs. the SNR_D at the destination node, obtained using the following strategies: a) Decode and forward using ML detector (dashed line) or sub-optimal detector: Theoretical value (solid line) and simulation results (circles); b) amplify and forward (dashed-dotted line); c) single hop (non-cooperative) case (dotted line). The block length is $N = 16$; the channels are simulated as FIR filters of order $L_h = 6$, whose taps are iid complex Gaussian random variables with zero mean and variance $1/d^2$. The SNR_R at the relay is equal to 20 dB. Comparing the D&F and A&F schemes, we observe that the D&F method performs better than the A&F at low and intermediate SNR_D values, but for high values of SNR_D , the A&F performs better. This shows that A&F is indeed a valuable choice.

V. COMPARISON AMONG ALTERNATIVE STC TECHNIQUES IN A MULTI-USER CONTEXT

In this section, we compare alternative DSTC strategies in a multi-user scenario. We consider a cell of radius 300 m with $N_{tot} = 200$ total radio terminals, located randomly. We consider only the uplink

¹⁴Differently from A&F scheme, in the D&F system there is no constraint on the sequence of information blocks transmitted from the source node.

¹⁵We drop the block index i for simplicity of notation, because the same relationships hold true for all blocks.

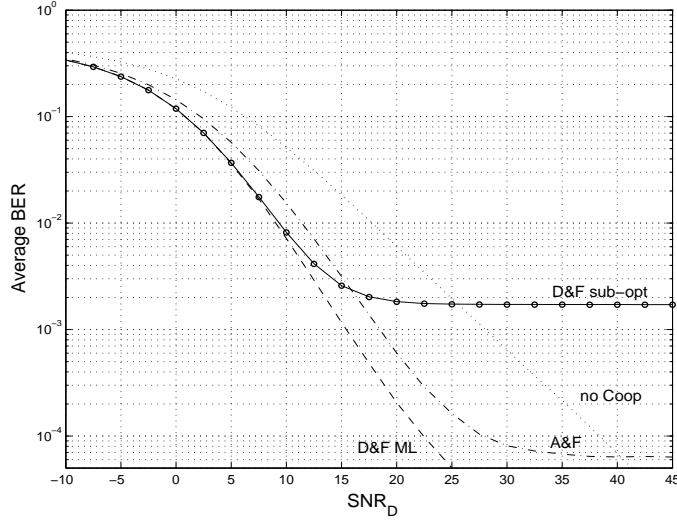


Fig. 13. Average BER vs. SNR_D (dB) achieved with different strategies: a) Decode and forward using ML detector (dashed line) or sub-optimal detector: Theoretical value (solid line) and simulation results (circles); b) amplify and forward (dashed-dot line); c) single hop (non-cooperative) case (dot line); $SNR_R = 20$ dB.

channel and we assume that the base station (destination) has two real antennas. Within the set of all radio terminals, $N = 10$ is the number of sources, whereas the remaining nodes are potential relays. All channels are slowly-varying, Rayleigh flat fading. The alternative strategies are compared enforcing the same overall radiated energy and the same bit rate in the SR2D phase. In case of cooperation, the energy includes the energy used to send data from the source to the relays and the sum of the energy used by source and relay to transmit their data to the destination. For each channel realization and radio nodes distribution, we associate a relay to a source according to the protocol described in Section II-D. We have used a 16-QAM constellation for the conventional SISO system, that acts as a benchmark term, while for the DSTC schemes the following choices have been made, in order to enforce the same bit rate in the SR2D phase:

- a) D-OSTC. As the symbol rate of the OSTC scheme is the same as a SISO system, the constellation used is the same, both if the sources finds a relay, and if it transmits alone. We have chosen 16-QAM so that each source transmits 8 bits every 22 symbol intervals. Two symbol intervals are reserved for the common S2R phase ($T_{S2R} = 2$) hence also in this phase 16-QAM is adopted.
- b) D-BLAST. A 4-QAM constellation is used in case of cooperation and a 16-QAM constellation

is used in case of no-cooperation.

The cooperative case can use a lower order constellation because a 2×2 D-BLAST provides a higher transmission rate.

- c) D-FDFR. A 4-QAM constellation is used in case of cooperation and a 16-QAM constellation is used in case of no-cooperation.

Also in this case, as with D-BLAST, the cooperative case can use a lower order constellation with respect to the non-cooperative case.

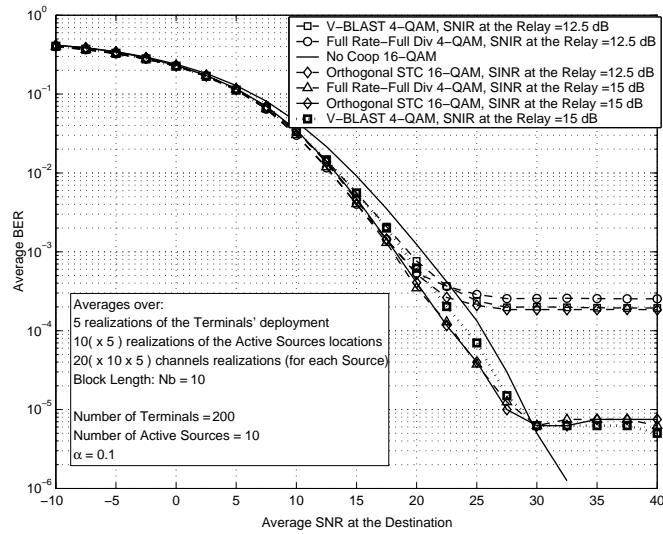


Fig. 14. BER comparison of different DSTC schemes

The simulation results are reported in Fig. 14. Throughout the simulations, the power used in the S2R slot is one tenth of the power used in the non-cooperative case. As explained in the last section, this portion could be optimized. A node is chosen as a relay if its Signal to Noise plus Interference Ratio (SNIR), conditioned to the channel, exceeds a threshold of 12.5 or 15 dB. Requiring a SNIR of 12.5 dB, a relay has been found with probability $p_R(1) = 0.72$, whereas for SNIR = 15 dB, we obtained $p_R(1) = 0.65$. Clearly, increasing the target SNIR, it decreases the probability of finding a relay, but, at the same time there are less decision errors at the relay. The overall performance is then a combination of these two aspects. The average BER reported in Fig. 14 takes into account both situations where the

relay has been found or not. We can check from Fig. 14 that indeed, increasing the SNIR from 12.5 to 15, even though $p_{r_0}(1)$ decreases, the floor on the BER decreases by more than a decade. Of course, this result is also a consequence of the relay density. Finally, in the case of a SNIR of 15 dB, we can observe a gain of approximately 3 dB at $BER = 10^{-4}$.

VI. COOPERATIVE SCHEME COMPOSED OF THE CASCADE OF SISO AND VIRTUAL MIMO LINKS

In this section, we focus on systems where the final destination has multiple antennas. This means that, if more relays cooperate with the source in sending information to the destination, we may establish a *virtual MIMO* link between the relays and the destination. The specific goal of this section is to derive the energy allocation and time sharing that provide a performance gain with respect to the non-cooperative case.

A non negligible issue is the geometry of the system, i.e., the relative location of the nodes involved in the communication. Aiming at establishing achievable rate limits, this aspect has been recently explicitly taken into account, in [70] for the Gaussian channel, in [71], for fading channels in the low-power regime, and in [72], where both an ergodic capacity analysis and an outage probability analysis are carried out for a one-relay channel, considering the effect, on the performance limits, of the relay location.

We consider a Rayleigh flat-fading channel in a scenario in which a source terminal exploits $n_R \geq 1$ relays to form a virtual array, thus enabling a MIMO transmission towards a final destination, which is equipped with $n_D \geq 1$ antennas. A sketch of the considered geometry is depicted in Fig. 15.

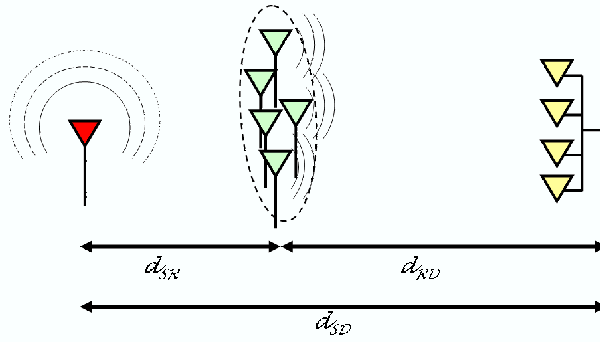


Fig. 15. Transmission through a virtual array of relays.

In this section, we establish the theoretical performance limits, both in the ergodic and non-ergodic case, emphasizing the dependence of these limits on the following parameters: *i*) the distances between

source, relays, and destination; *ii)* the power allocation and *iii)* the time allocation, between the two phases.

In the *general* case, the destination can receive signals in both the transmission phases. Furthermore, the source may participate to the MIMO phase, thus contributing to the system diversity. For simplicity, however, we will assume that the source transmits in the first phase only, and the destination receives in the second phase only. Thus, we have the cascade of a *one-to-many* link between the source and the relays, which we will call a n_R -SISO channel, and a MIMO link between the virtual array of relays and the physical array at destination. The significance of our result is not affected by this simplifying assumption, since it clearly represents a worst-case scenario, with respect to the general case.

Throughout this section, we shall assume decode & forward, [53], as the relaying mode. Our goal is to show that a MIMO communication can be effectively implemented with single-antenna transmitters, thus yielding the well known benefits of MIMO systems. Special emphasis will be given to the role of the geographical distribution of the relays, power allocation and time-sharing.

Both in the ergodic and non-ergodic cases, we will compare the performance limits of the proposed system with those of a traditional direct source-destination SIMO link.

1) System model and problem formulation: We assume that the source is equipped with a single physical antenna, whereas the destination is equipped with an array of n_D antennas. In between, there is a set of n_R single-antenna relays, that assist the source in the transmission, through the formation of a virtual array. In our setup the relays do not have their own data to send. The communication is divided in two phases: in the first phase, that we call the “source to relays” (*S2R*) phase, the source sends its data to the relays in a broadcast fashion. The relays receive and decode the data and, in the second phase, called the “relays to destination” (*R2D*) phase, transmit the data to the destination as in a MIMO link. Since the scope of our analysis, at this stage, is not to find the best suitable transmission strategy, but to investigate the information-theoretical limits of the proposed protocol, we do not assume a specific space-time code for the *R2D* phase. However, we will assume that in order to achieve full diversity, all the relays must decode the entire set of data in the first phase, thus enabling the use of full diversity schemes in the second phase.

We assume a Rayleigh flat-fading channel in all the links. The discrete-time channel between the source and one of the relays (*S2R*), is modeled by the input/output relation

$$y_{r,k} = \sqrt{\frac{\mathcal{P}_S}{(1 + d_k^\eta)}} h_k x + w, \quad (53)$$

where \mathcal{P}_S is the transmission power, h_k is a complex gaussian random variable with zero mean and unit

variance that represents the normalized channel coefficient, d_k is the distance¹⁶ between the source and the k -th relay, η is the path loss exponent, x is the transmitted symbol, assumed to have unit energy, i.e. $E\{|x|^2\} = 1$, and finally w is an additive white complex Gaussian noise term with zero mean and variance σ^2 .

In the $R2D$ phase, the MIMO link between the relays and the destination is modeled by the input/output relation

$$\mathbf{z} = \sqrt{\frac{\mathcal{P}_R}{n_R}} \mathbf{H} \mathbf{D} \tilde{\mathbf{y}} + \mathbf{w}, \quad (54)$$

where \mathbf{z} is the n_D -size received vector, $\tilde{\mathbf{y}}$ is a vector whose k -th entry represents the symbol transmitted by the k -th relay, which depends on what the relay has received in the first phase, \mathcal{P}_R is the transmit power, which is equally divided among the relays, \mathbf{w} is an n_D -size additive noise vector with independent zero mean circularly symmetric Gaussian entries of variance σ^2 , \mathbf{H} is the $n_D \times n_R$ normalized channel matrix, whose elements are i.i.d. circularly symmetric complex Gaussian random variables with zero mean and unit variance, finally, \mathbf{D} is a $n_R \times n_R$ diagonal matrix that takes into account the average path losses, and is defined as

$$\mathbf{D} diag \left(\left(1 + d_{D,1}^\eta \right)^{-1/2}, \dots, \left(1 + d_{D,n_R}^\eta \right)^{-1/2} \right), \quad (55)$$

where $d_{D,k}$, $k = 1, \dots, n_R$, are the distance between the relays and the destination, and η is the path loss exponent, usually in the interval [2, 6].

We assume that the source sends a total of M_b bits to the destination in an interval of T channel uses, i.e., at an *average* transmission rate of $R = M_b/T$ bits per channel use (bpcu). T_{S2R} channel uses will be employed for the $S2R$ phase, whereas T_{R2D} channel uses are reserved for transmission between the relays and the destination. We define ε as the total energy, comprehensive of both the $S2R$ and the $R2D$ phases, employed to send the data to destination. The *average* power is given by

$$\mathcal{P}_{av} \frac{\varepsilon}{T}. \quad (56)$$

We assume that a fraction α of the total energy is employed in the first phase, and the remaining fraction $(1 - \alpha)$ is reserved for the second phase. The power term \mathcal{P}_S in (53) becomes

$$\mathcal{P}_S = \alpha \frac{\varepsilon}{T_{S2R}} = \left(\alpha \frac{T}{T_{S2R}} \right) \mathcal{P}_{av}. \quad (57)$$

¹⁶Notice that with the propagation model assumed in (53), the distance is normalized so that a unit distance corresponds to the distance at which the transmission power is halved.

Since in the $S2R$ phase the relays have to receive M_b bits, the rate of SISO links of the $S2R$ phases is given by

$$R_{S2R} \frac{M_b}{T_{S2R}} = \frac{T}{T_{S2R}} R. \quad (58)$$

Similarly to (57), we define the average power employed in the $R2D$ phase, that appears in (54), as

$$\mathcal{P}_D = (1 - \alpha) \frac{\varepsilon}{T_{R2D}} = \left((1 - \alpha) \frac{T}{T_{R2D}} \right) \mathcal{P}_{av}, \quad (59)$$

whereas the rate of the virtual MIMO channel is

$$R_{S2R} \frac{M_b}{T_{R2D}} = \frac{T}{T_{R2D}} R. \quad (60)$$

In the following, we will assess the performance limits of this communication system, comparing them with those achievable with a standard direct link between the source and the destination. We will consider two different channel evolution models, i.e. ergodic and non-ergodic fading channels. Transmission over ergodic channels means that the channel coherence time is sufficiently short to encode the information in codewords that last across many independent channel realization. Clearly, the channel coherence time should in any case be sufficiently long to enable CSI acquisition at the receiver. For ergodic channels, it is possible to define the *capacity* in the classical formulation, as the maximum information rate that the channel can support enabling, in principle, an almost error-free communication. Non-ergodic fading channels refer instead to a very slow fading environment in which, due to delay constraints, coding over multiple channel realization is impossible. Thus, for every channel realization it is possible to define a supported rate, or “*instantaneous capacity*”, but it is known that the capacity of the channel, in the Shannon sense, is zero. In this case the performance limits are conveniently expressed in terms of *outage probability*, with reference to a given target information rate R , or *outage capacity*, with reference to a given outage probability P_{out} . The first is defined as the probability that the instantaneous capacity, which is a random variable, is less than the required rate. The second is the rate that guarantees that the probability that a single channel realization can support it is less or equal to the desired P_{out} .

The scope of our analysis is to emphasize the role played by the parameters introduced in (53)-(60), namely: the (relative) distances between the relays and the source/destination, d_k , $d_{D,k}$, $k = 1, \dots, n_R$, the power allocation across the two phases, represented by the parameter α , and the time division of the two phases represented by the ratio T/T_{S2R} .

We examine now the ergodic case.

2) *Ergodic capacity analysis:* If the system requirements on the decoding delay allow for a coded blocklength which is much greater than the channel coherence time, each block has the possibility to be reliably decoded, if the transmission rate is below the *ergodic channel capacity*. For the *S2R* phase, the capacity of the link between the source and the k -th relay, measured in bits per channel use, is given by

$$\bar{C}_{S2R,k} = E_{\xi_k} \left\{ \log \left(1 + \frac{\mathcal{P}_S}{\sigma^2} \xi_k \right) \right\}, \quad k = 1, \dots, n_R, \quad (61)$$

where $\xi_k |h_k|^2 / (1 + d_k^\eta)$, $k = 1, \dots, n_R$, are the path losses corresponding to a single channel realization on the n_R links. It is easy to check that the path losses are exponentially distributed random variables with parameters $(1 + d_k^\eta)$, $k = 1, \dots, n_R$, respectively.

Since for an end-to-end reliable communication it is necessary that all the relays perfectly decode the transmitted codeword, we can define an overall capacity in the *S2R* link, which is the minimum among all the capacities of the n_R parallel channels

$$\bar{C}_{S2R} = \min \{ \bar{C}_{S2R,1}, \dots, \bar{C}_{S2R,n_R} \}. \quad (62)$$

In the *D2R* phase, we have a MIMO link whose ergodic capacity is given by

$$\bar{C}_{R2D} = E_H \left\{ \log \det \left(\mathbf{I}_m + \frac{\mathcal{P}_R}{n_R \sigma^2} \mathbf{W} \right) \right\}, \quad (63)$$

where $m \min(n_R, n_D)$, \mathbf{I}_m is the Identity matrix of size m , and \mathbf{W} is defined as

$$\mathbf{W} \begin{cases} \mathbf{H}\mathbf{D}(\mathbf{H}\mathbf{D})^H, & \text{if } n_R \geq n_D \\ (\mathbf{H}\mathbf{D})^H \mathbf{H}\mathbf{D}, & \text{if } n_R < n_D \end{cases}. \quad (64)$$

We have that if $\bar{C}_{S2R} \geq \bar{C}_{R2D}$, the maximum information that could be, in principle, transferred to the relays, cannot flow toward the destination because the MIMO channel is not able to support it. Viceversa, if $\bar{C}_{R2D} \geq \bar{C}_{S2R}$, it is clear that the bottleneck for the information flow lies in the first link. The capacity of the composite link we are considering is hence given by the minimum among the two:

$$\bar{C}_{S2D} = \min \{ \bar{C}_{S2R}, \bar{C}_{R2D} \}. \quad (65)$$

For the sake of simplicity, let us assume that the relays are located at the same distance from the source, i.e. $d_k = d_{SR}$, $k = 1, \dots, n_R$, and also from the destination, i.e. $d_{D,k} = d_{RD}$, $k = 1, \dots, n_R$.

We also assume that the relays lay on the direction connecting the source to the destination, as depicted in Fig. 15, i.e.

$$d_{RD} + d_{SR} = d_{SD}. \quad (66)$$

In this case we have:

$$\mathbf{W} = (1 + (d_{SD} - d_{SR})^\eta)^{-1} \widetilde{\mathbf{W}}, \quad (67)$$

where

$$\widetilde{\mathbf{W}} \begin{cases} \mathbf{H}\mathbf{H}^H, & \text{if } n_R \geq n_D \\ \mathbf{H}^H\mathbf{H}, & \text{if } n_R < n_D \end{cases}. \quad (68)$$

From (61) and (63) we can rewrite the capacities in the two phases, by making explicit the dependence on the distances d_{RD} , d_{SR} , and d_{SD} , on the power allocation and time-sharing, represented by α and the ratio T/T_{S2R} , respectively, thus obtaining

$$\bar{C}_{S2R} = \frac{T_{S2R}}{T} E_h \left\{ \log \left(1 + \left(\alpha \frac{T}{T_{S2R}} \right) \frac{\mathcal{P}_{av}}{\sigma^2} \frac{|h|^2}{(1 + d_{SR}^\eta)} \right) \right\} \quad (69)$$

$$\bar{C}_{R2D} = \frac{T_{R2D}}{T} E_H \left\{ \log \left| \mathbf{I}_m + \frac{\left((1 - \alpha) \frac{T}{T_{R2D}} \right) \mathcal{P}_{av}}{n_R \sigma^2 (1 + (d_{SD} - d_{SR})^\eta)} \widetilde{\mathbf{W}} \right| \right\}, \quad (70)$$

where we have introduced the scale factors T_{S2R}/T and T_{R2D}/T , for a fair comparison with a direct transmission system. We can see that, for a given distance d_{SD} between the source and the destination, the effect of an increase in d_{SR} is to increase \bar{C}_{R2D} and to decrease \bar{C}_{S2R} , thus, we can expect that there will be a value d_{SR}^* of the distance for which the two capacities are equal and yield the maximum achievable rate of the system. Furthermore, the capacity is also increased, or decreased, depending on the power allocation and the transmission time allocation.

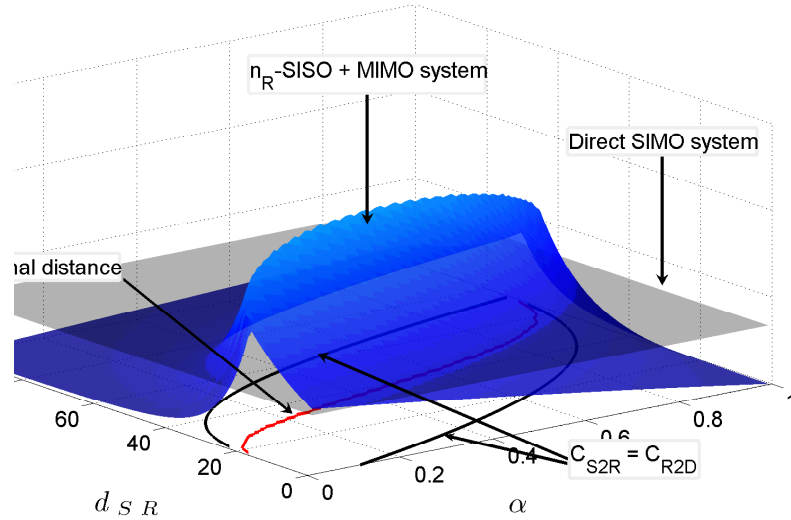


Fig. 16. Ergodic capacity of the cooperative system, compared with the capacity of a direct S→D transmission system

In Fig. 16 we have plotted the ergodic capacity of a cooperative system (blue surface) formed by $n_R = 6$ relays and a receiver with $n_D = 3$ antennas. The black surface represent the ergodic capacity

of the direct system, the red curve represents the distance that maximizes the capacity, for each value of α , whereas the region of the (α, d_{SR}) plane comprised between the two black contours is the region of distances for which the cooperative system outperforms the direct system. These results were obtained with $d_{SD} = 100$, $\eta = 3$, and $\mathcal{P}_{av}/\sigma^2 = 100 \text{ dB}$, and a time-sharing factor $T_{S2R}/T = 0.5$.

We can see that there exist range of values of α and d_{SR} providing a significant benefit over the SIMO channel between source and destination, thus justifying the use of cooperative relaying. It is important, however to choose properly the value of α for a given distance (or viceversa) to achieve the best performance. Similar results would be obtained for a fixed α , and different values of the time-sharing factor.

3) *Outage based analysis:* Depending on the channel coherence time, it could be impractical to send code-blocks whose length allows to achieve the ergodic capacity \bar{C} of the fading channel. In a slow fading scenario, it is frequent to consider the single channel realizations and evaluate the performance in terms of outage capacity or outage probability. In practice, each channel realization yields a realization of a random variable, called “*instantaneous capacity*”, C_h (see for example [59]), which is the capacity, in the Shannon sense, that one would have if that channel realization had an infinite duration. If the duration of the channel realization is sufficiently long, one can think to coded-blocks of length sufficient to achieve an (almost) error-free transmission. If this is the case, it is known that the probability of an erroneous transmission, for a given *transmission rate* R , is dominated by the outage probability on that link, i.e. the probability that C_h , which is now a random variable, is less than the desired rate.

$$P_{out} \Pr \{C_h \leq R\}. \quad (71)$$

In this section we derive an expression of the outage probability of the system described in section VI-1 with special emphasis on the geometry of the system, i.e. on the relative distances between the source, the relays, and the destination, and on the power balance between the *S2R* phase and the *R2D* phase. We then compare the obtained result with the outage probability of a system which employs direct transmission between the source and the destination.

In order to obtain the desired result, we will first calculate the outage probability in the *S2R* phase, $P_{out,S2R}$, defined as the probability that at least one of the n_R independent links between the source and the relays is in outage with respect to R . The first result on $P_{out,S2R}$ will be general, in the sense that it will be a function of the n_R (possibly different) distances, d_1, \dots, d_k , between source and relays. Subsequently, we shall assume that the relays are located at the same distance, d_{SR} , from the source, and also that the distance between the relays and the destination is (approximately) the same, thus referring

to a situation as the one depicted in Fig. 15. This assumption will simplify our successive analysis of the outage probability in the *R2D* phase, $P_{out,R2D}$, and of the end-to-end link, $P_{out,TOT}$, that we carry out in paragraphs (VI.-4.a) and (VI.-4.b). Thanks to this assumption we can single out the effect of both the relative distance between the source, the relays and the destination, and of the power balance between the two phases.

4) *Source to relays outage probability*: Let us consider the link between the source and one, say the k -th, of the relays. The *instantaneous capacity* of this *SISO* link, measured in bits per channel use (bpcu), is given by the term inside the expectation operator in (61), i.e.

$$C_{S2R,k} = \log \left(1 + \frac{\mathcal{P}_S}{\sigma^2} \frac{|h_k|^2}{(1 + d_k^\eta)} \right) \quad (72)$$

$$= \log \left(1 + \frac{\mathcal{P}_S}{\sigma^2} \xi_k \right), \quad k = 1, \dots, n_R \quad (73)$$

where \mathcal{P}_S is the transmission power. For this link, the *outage event* for a given “*target information rate*” of R bpcu, is defined as

$$C_{S2R,k} \leq R. \quad (74)$$

It is easy to see that the outage events (74) can be expressed as

$$\xi_k \leq (2^R - 1) \frac{\sigma^2}{\mathcal{P}_S}, \quad k = 1, \dots, n_R. \quad (75)$$

We define the outage probability in the *S2R* phase, as the probability of the union of the outage events on the single links. It is sufficient that one of the links is in outage to have an outage in this phase. Equivalently, an outage occurs if (at least) the minimum among all the instantaneous capacities of the *S2R* links is less than the required rate R , i.e.

$$P_{out,S2R} \Pr \{ \min(C_{S2R,1}, \dots, C_{S2R,n_R}) \leq R \}. \quad (76)$$

Since the instantaneous capacities (72) are monotone increasing functions of the respective path losses, we can equivalently write

$$P_{out,S2R} = \Pr \left\{ \min(\xi_1, \dots, \xi_{n_R}) \leq (2^R - 1) \frac{\sigma^2}{\mathcal{P}_S} \right\}. \quad (77)$$

Due to the assumptions on the (normalized) fading channel coefficients h_k , $k = 1, \dots, n_R$, we have that ξ_1, \dots, ξ_k are statistically independent exponential random variables with parameter

$$\lambda_k (1 + d_k^\eta), \quad k = 1, \dots, n_R. \quad (78)$$

We define now

$$\xi \min(\xi_1, \dots, \xi_{n_R}). \quad (79)$$

It is known that the minimum in a set of independent exponential random variables is itself exponential, with parameter equal to the sum of the parameters. Hence ξ is exponential with parameter

$$\lambda \sum_{k=1}^{n_R} \lambda_k = \sum_{k=1}^{n_R} (1 + d_k^\eta). \quad (80)$$

From (77) we have

$$\begin{aligned} P_{out,S2R} &= \Pr \left\{ \xi \leq (2^R - 1) \frac{\sigma^2}{\mathcal{P}_S} \right\} \\ &= 1 - e^{-\lambda(2^R-1)\frac{\sigma^2}{\mathcal{P}_S}}. \end{aligned} \quad (81)$$

Let us now assume that all the relays are located at the same distance d_{SR} from the source, i.e.

$$d_k = d_{SR}, \quad k = 1, \dots, n_R. \quad (82)$$

In this case it is easy to show that the outage probability (81) becomes

$$P_{out,S2R} = 1 - e^{-n_R(1+d_{SR}^\eta)(2^R-1)\frac{\sigma^2}{\mathcal{P}_S}}. \quad (83)$$

In the sequel we will use this expression to evaluate the end-to-end outage probability. We now turn our attention to the *R2D* phase.

a) Relays to destination outage probability: If the data sent from the source have been perfectly decoded by the all the n_R relays, we end up with a set of terminals that have the same data and may then cooperate to transmit them to the destination. In practice, the set of relays can be viewed as an antenna array, and the channel between this array and the destination, as a MIMO channel. As for the SISO channel, we consider the capacity given by a single channel realization:

$$C_{R2D} = \log \det \left(\mathbf{I}_m + \frac{\mathcal{P}_R}{n_R \sigma^2} \mathbf{W} \right), \quad (84)$$

with \mathbf{W} defined in (64).

Under the simplifying assumption that all the relays are at the same distance d_{RD} from the destination, the diagonal matrix \mathbf{D} becomes a multiple of the identity matrix of size n_R , i.e. $\mathbf{D} = (1 + d_{RD}^\eta)^{-1/2} \mathbf{I}_{n_R}$. In this case, the entries of the matrix $\mathbf{H}\mathbf{D}$ are identically distributed, and \mathbf{W} acquires the expression in (67).

It is hard to obtain a closed form expression for the probability density function of the instantaneous capacity. However, in literature, several asymptotic analyses have been carried out, that provide a useful mean to obtain an (albeit approximate) expression of the outage probability. We refer to the asymptotic expression, for the distribution of the instantaneous capacity, derived in [59] (see also the reference therein).

More specifically, introducing the following quantities

$$\omega \sqrt{\frac{\sigma^2 (1 + d_{RD}^\eta)}{P_R}} \quad (85)$$

$$\beta \frac{n_D}{n_R} \quad (86)$$

$$q_0 \frac{\beta - 1 - \omega^2 + \sqrt{(\beta - 1 - \omega^2)^2 + 4\omega^2\beta}}{2\omega} \quad (87)$$

$$r_0 \frac{1 - \beta - \omega^2 + \sqrt{(1 - \beta - \omega^2)^2 + 4\omega^2}}{2\omega}, \quad (88)$$

it can be shown that as the number of transmitting and receiving antennas goes to infinity, and the ratio $\beta = n_D/n_R$ tends to a constant, the instantaneous capacity tends to be distributed as a Gaussian random variable,

$$C_{R2D} \sim \mathcal{N}(\mu_C, \sigma_C^2), \quad (89)$$

with the mean and variance given by

$$\begin{aligned} \mu_C &= n_R \{ (1 + \beta) \log \omega + q_0 r_0 \log e \\ &\quad + \log r_0 + \beta \log (q_0/\beta) \} \end{aligned} \quad (90)$$

$$\sigma_C^2 = \log e \log \left(1 - \frac{q_0^2 r_0^2}{\beta} \right). \quad (91)$$

In practice, the asymptotic mean and variance of C_{R2D} yield a close approximation to the statistics of C_{R2D} even for very small n_R and n_D .

Therefore, the outage probability in the $R2D$ section of the link, with respect to the required rate R , can be approximated with the Gaussian Q -function, as follows:

$$P_{out,R2D} \simeq Q \left(\frac{\mu_C - R}{\sigma_C^2} \right). \quad (92)$$

It is shown in [59] that this expression gives a close approximation to the actual $P_{out,R2D}$ even at very small values. In the following paragraph we exploit the results on the two phases of the transmission to obtain an expression for the outage probability of the whole system.

b) End to end outage probability: The end-to-end communication link is the cascade of the $S2R$ and the $R2D$ links. With the setup of section VI-1, to guarantee that the information, that flows through the two links, can be perfectly recovered at the destination, it is necessary that none of the two links is

in outage, otherwise the information is destroyed and cannot be recovered. Since, for a given rate, the outage events in the two links are independent, it is easy to show that the outage probability is given by:

$$P_{out,TOT} = P_{out,S2R} + P_{out,R2D} - P_{out,S2R}P_{out,R2D}. \quad (93)$$

Assuming that the relays are located at a distance d_{SR} from the source and on the line connecting the source with the destination, as in Fig. 15, the distance between the relays and the destination is given by

$$d_{RD} = d_{SD} - d_{SR}. \quad (94)$$

Combining (93), (83), and (92), we obtain:

$$P_{out,TOT} = 1 - e^{-n_R(1+d_{SR}^\eta)(2^R-1)\frac{\sigma^2}{\alpha T_{S2R} \mathcal{P}_{av}}} \quad (95)$$

$$+ Q\left(\frac{\mu_C - R}{\sigma_C^2}\right) \quad (96)$$

$$- \left(1 - e^{-\frac{n_R(1+d_{SR}^\eta)(2^R-1)}{\alpha T_{S2R} \frac{\mathcal{P}_{av}}{\sigma^2}}}\right) Q\left(\frac{\mu_C - R}{\sigma_C^2}\right). \quad (97)$$

This expression depends on the distances, on the power allocation, represented by the parameter α , and on the ratio between the total transmission interval and the sub-intervals reserved for the $S2R$ and the $R2D$ phases. Notice that now μ_C and σ_C^2 are related to this quantities through $\mathcal{P}_R = (1 - \alpha) \frac{T}{T_{D2R}} \mathcal{P}_{av}$, and $d_{RD} = d_{SD} - d_{SR}$.

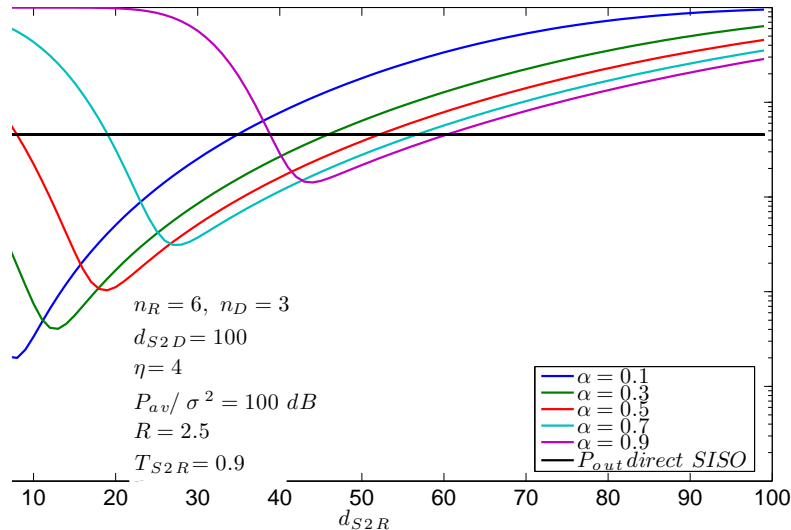


Fig. 17. Outage probability of the cooperative system (colored lines) versus the outage probability of a direct SIMO link.

In Fig. 17 we have plotted the outage probability obtained with the relayed transmission, and the outage probability of the direct transmission. It was assumed that the destination was equipped with an array of $n_D = 3$ antennas, and $n_R = 6$ relays were employed for cooperation. The distance between the source and the destination was $d_{SD} = 100$, and the path loss exponent $\eta = 4$. The ratio between the average *transmit* power and the noise variance at the receivers, $\mathcal{P}_{av}/\sigma^2$, was 100 dB, and the time-sharing factor was $T_{S2R}/T = 0.9$. Different curves refer to different values of the power allocation parameter α . We can see that, for a given power allocation α , there is an optimal location of the relays, whereas for a given location of the relays, the power allocation can be adjusted to obtain the best gain over the direct transmission system.

In this case we can see that, for a relay location up to halfway between the source and the destination, there exist a power allocation that yields a significant gain over the direct system.

VII. CONCLUSION

In conclusion, distributed space-time coding can be an important tool to reduce the overall radiated power in wireless networks. We have considered here only the case with two hops, but further improvements may be expected in the multi-hop case. The price paid for these advantages is the additional signaling required to coordinate the transmission of source and relay nodes, an important issue which is currently under investigation.

REFERENCES

- [1] F. Tobagi, "Modeling and performance analysis of multihop packet radio networks," *Proc. of the IEEE*, vol. 75, no. 1, pp. 135–155, 1987.
- [2] T. M. Cover and A.A. El Gamal, "Capacity theorems for the relay channel", *IEEE Trans. Inform. Theory*, pp. 572–584, Sept. 1979.
- [3] H. Bolcskei, R.U. Nabar, O. Oyman, A.J. Paulraj, "Capacity scaling laws in MIMO relay networks," *IEEE Trans. on Wireless Communications*, pp. 1433–1444, June 2006.
- [4] M. Gastpar, M. Vetterli, "On the capacity of large Gaussian relay networks," *IEEE Trans. on Information Theory*, pp. 765–779, March 2005.
- [5] G. Kramer, M. Gastpar, P. Gupta, "Cooperative Strategies and Capacity Theorems for Relay Networks", *IEEE Trans. on Information Theory*, pp. 3037–3063, Sept. 2005.
- [6] A. Paulraj, R. Nabar, and D. Gore, *Introduction to space-time wireless communications*, Cambridge, UK: Cambridge University Press, 2003.
- [7] E. G. Larsson and P. Stoica, *Space-time block coding for wireless communications*, Cambridge, UK: Cambridge University Press, 2003.

- [8] P. Gupta and P. R. Kumar, "Critical power for asymptotic connectivity in wireless networks", in *Stochastic Analysis, Control, Optimization and Applications*, pp. 547-566, Birkhäuser Boston, Boston, Mass., USA, 1999.
- [9] Gilbert, E.N., "Random plane networks," 1961, *SIAM J.*, vol. 9, pp. 533–543.
- [10] Booth, L., Bruck, J., Franceschetti, M., Meester, R., "Covering algorithms, continuum percolation and the geometry of wireless networks," *The Annals of Applied Probability*, No. 2, 2003, pp. 722–741.
- [11] Penrose, M. D., "On k -connectivity for a geometric random graph," *Wiley Random Structures and Algorithms*, vol. 15, no. 2, 1999, pp.145–164.
- [12] Bettstetter, C., "On the minimum node degree and connectivity of a wireless multihop network," *Proc. of MOBIHOC '02*, EPF Lausanne, 16-20 June 2002, pp. 80–91.
- [13] D. Miorandi, E. Altman, "Coverage and connectivity of ad hoc networks in presence of channel randomness," *Proc. of INFOCOM 2005*, Miami, March 13–17, 2005.
- [14] P. Gupta and P. R. Kumar, "The capacity of wireless networks," *IEEE Trans. Inform. Theory*, vol. 46, no.2, pp. 388–404, 2000.
- [15] A. Host-Madsen, "On the capacity of wireless relaying," in *Proc. IEEE 56th Vehicular Technology Conference (VTC 2002-Fall)*, vol. 3, pp. 1333 -1337, Vancouver, BC, Canada, September 2002.
- [16] A. Sendonaris, E. Erkip, and B. Aazhang, "Increasing uplink capacity via user cooperation diversity", in *Proc. IEEE International Symposium on Information Theory (ISIT '98)*, p. 156, Cambridge, Mass, USA, August 1998.
- [17] J.N. Laneman and G.W. Wornell, "Energy-efficient antenna sharing and relaying for wireless networks", in *Proc. IEEE Wireless Communications and Networking Conference (WCNC '00)*, vol. 1, pp. 7–12, Chicago, Ill, USA, September 2000.
- [18] J. N. Laneman and G. W. Wornell, "Distributed space-time coded protocols for exploiting cooperative diversity in wireless networks", in *Proc. IEEE Global Telecommunications Conference (GLOBECOM '02)*, vol. 1, pp. 77–81, Taipei, Taiwan, November 2002.
- [19] J. N. Laneman and G. W. Wornell, "Distributed space-time-coded protocols for exploiting cooperative diversity in wireless networks", *IEEE Trans. Inform. Theory*, vol. 49, no. 10, pp. 2415–2425, 2003.
- [20] V. Emamian, M. Kaveh, "Combating shadowing effects for systems with transmitter diversity by using collaboration among mobile users", in *Proc. of International Symposium on Communications (ISCOM '01)*, vol. 9.4, pp. 105.1–105.4, Taiwan, November 2001.
- [21] T.E. Hunter, A. Nosratinia, "Cooperation diversity through coding", in *Proc. IEEE International Symposium on Information Theory (ISIT '02)*, p. 220, Lausanne, Switzerland, June-July 2002.
- [22] M. Dohler, E. Lefranc, H. Aghvami, "Space-time block codes for virtual antenna arrays", in *Proc. 13th IEEE International Symposium on Personal, Indoor, and Mobile Radio Communications (PIMRC '02)*, vol.1, pp. 414–417 , Lisbon, Portugal, September 2002.
- [23] A. Stefanov, E. Erkip, "Cooperative coding for wireless networks", in *Proc. 4th International Workshop on Mobile and Wireless Communications Network*, pp. 273–277, Stockholm, Sweden, September 2002.
- [24] I. Hammerstroem, M. Kuhn, B. Rankov, A. Wittneben, "Space-time processing for cooperative relay networks", in *Proc. IEEE 58th Vehicular Technology Conference (VTC 2003-Fall)*, vol. 1, pp. 404–408, Orlando, Fla, USA, October 2003.
- [25] P. A. Anghel, G. Leus, M. Kaveh, "Multi-user space-time coding in cooperative networks," in *Proc. 28th IEEE International Conference on Acoustics, Speech, and Signal Processing (ICASSP '03)*, vol. 4, pp. IV-73-IV-76, Hong Kong, April 2003.
- [26] S. Barbarossa, G. Scutari, "Cooperative diversity through virtual arrays in multihop networks," in *Proc. 28th IEEE*

- International Conference on Acoustics, Speech, and Signal Processing (ICASSP '03)*, vol. 4, pp. IV-209–IV-212, Hong Kong, April 2003.
- [27] G. Scutari, S. Barbarossa, D. Ludovici, “Cooperation diversity in multihop wireless networks using opportunistic driven multiple access”, in *Proc. 4th IEEE Workshop on Signal Processing Advances in Wireless Communications (SPAWC '03)*, pp. 170–174, Rome, Italy, June 2003.
- [28] S. Barbarossa, G. Scutari, “Distributed space-time coding strategies for wideband multihop networks: Regenerative vs. non-regenerative relays”, in *Proc. 29th IEEE International Conference on Acoustics, Speech, and Signal Processing (ICASSP '04)*, vol. 4, pp IV-501–IV-504, Montreal, Canada, May 2004.
- [29] S. Barbarossa, G. Scutari, “Distributed space-time coding for multihop networks”, in *Proc. IEEE International Conference on Communications (ICC '04)*, vol. 2, pp. 916–920, Paris, France, June 2004.
- [30] S. Barbarossa, L. Pescosolido, D. Ludovici, L. Barbetta, G. Scutari, “Cooperative wireless networks based on distributed space-time coding”, in *Proc. IEEE International Workshop on Wireless Ad-Hoc Networks (IWWAN '04)*, Oulu, Finland, May 31-June 3, 2004.
- [31] N. A. C. Cressie, *Statistics for Spatial Data*, John Wiley & Sons, New York, NY, USA, 1993.
- [32] M. K. Simon and M.-S. Alouini, *Digital communications over fading channels: A unified approach to performance analysis*, John Wiley & Sons, New York, NY, USA, 2000.
- [33] J. Proakis, *Digital Communications*, McGraw Hill, New York, NY, USA, 4th edition, 2000.
- [34] H. El Gamal and M. O. Damen, “Universal space-time coding”, *IEEE Trans. Inform. Theory*, vol. 49, no. 5, pp. 1097–1119, 2003.
- [35] X. Ma and G. B. Giannakis, “Full-diversity full-rate complex-field space-time coding”, *IEEE Trans. Signal Processing*, vol. 51, no. 11, pp. 2917–2930, 2003.
- [36] L. Zheng and D. N. C. Tse, “Diversity and multiplexing: A fundamental tradeoff in multiple antenna channels,” *IEEE Trans. Inform. Theory*, vol. 49, no. 5, pp. 1073–1096, 2003.
- [37] G.J. Foschini, “Layered Space-Time architecture for Wireless Communication in a fading environment when using multiple antennas”, *Bell Labs Tech. Journal*, vol. 1, no. 2, pp. 41-59, 1996.
- [38] S. Barbarossa and A. Fasano, “Trace-orthogonal space-time coding design for multiuser systems”, in *Proc. 30th IEEE International Conference on Acoustics, Speech, and Signal Processing (ICASSP '05)*, vol. III, pp. III-1093–III-1096, Philadelphia, PA, March 2005.
- [39] S. Barbarossa and F. Cerquetti, “Simple space-time coded SS-CDMA systems capable of perfect MUI/ISI elimination”, *IEEE Commun. Lett.*, vol. 5, no. 12, pp. 471–473, 2001.
- [40] G. Scutari and S. Barbarossa, “Distributed Space-Time Coding for Regenerative Relay Networks”, *IEEE Trans. Wireless Communications*, to appear, 2005.
- [41] K. Cho and D. Yoon, “On the general BER expression of one- and two-dimensional amplitude modulations ”, *IEEE Trans. Commun.*, vol. 50, no. 7, pp. 1074 – – 1080, 2002.
- [42] A. Stefanov and E. Erkip, “On the performance analysis of cooperative space-time coded systems”, in *Proc. IEEE Wireless Communications and Networking Conference (WCNC '03)*, vol. 2, pp. 729–734, New Orleans, La, USA, March 2003.
- [43] P. A. Anghel, G. Leus, and M. Kaveh, “Relay assisted uplink communication over frequency-selective channels”, in *Proc. 4th IEEE Workshop on Signal Processing Advances in Wireless Communications (SPAWC '03)*, pp. 125–129, Rome, Italy, June 2003.

- [44] T.E. Hunter and A. Nosratinia, "Performance analysis of coded cooperation diversity", in *Proc. IEEE International Conference on Communications (ICC '03)*, Vol. 4, pp. 2688–2692, Anchorage, Alaska, USA, May 2003.
- [45] B. Bollobás, *Modern Graph Theory*, vol 184 of *Graduate Texts in Mathematics*, Springer-Verlag, New York, NY, USA, 1998.
- [46] M. D. Penrose, *Random Geometric Graphs*, vol. 5 of *Oxford Studies in Probability*, Oxford University Press, Oxford, UK, 2003.
- [47] C. Bettstetter, "On the minimum node degree and connectivity of a wireless multihop network", in *Proc. 3rd ACM International Symposium on Mobile Ad Hoc Networking and Computing (MOBIHOC '02)*, pp. 80–91, Lausanne, Switzerland, June 2002.
- [48] M. D. Penrose, "On k -connectivity for a geometric random graph", *Wiley Random Structures and Algorithms*, vol. 15, no. 2, pp.145–164, 1999.
- [49] Y.-C. Cheng and T. G. Robertazzi, "Critical connectivity phenomena in multihop radio models", *IEEE Trans. Commun.*, vol. 37, no. 7, pp 770–777, 1989.
- [50] S. Barbarossa, "Multiantenna Wireless Communication Systems", Artech House Publishers, Norwood, Mass., USA, March 2005.
- [51] A. Sendonaris, E. Erkip, and B. Aazhang, "User Cooperation Diversity—Part I: System Description," *IEEE Trans. Commun.*, vol. 51, no. 11, pp. 1927–1938, Nov. 2003.
- [52] J. N. Laneman and G. W. Wornell, "Distributed Space–Time-Coded Protocols for Exploiting Cooperative Diversity in Wireless Networks," *IEEE Trans. Inform. Theory*, vol. 49, no. 10, pp. 2415–2425, Oct. 2003.
- [53] J. N. Laneman, D. N. C. Tse, and G. W. Wornell, "Cooperative Diversity in Wireless Networks, Efficient Protocols and Outage Behavior," *IEEE Trans. Inform. Theory*, vol. 50, no. 12, pp. 3062–3080, Dec. 2004.
- [54] A. Nosratinia, T. E. Hunter, and A. Hedayat, "Cooperative Communications in Wireless Networks," *IEEE Commun. Mag.*, vol. 42, no. 10, pp. 74–80, Oct. 2004.
- [55] T. E. Hunter and A. Nosratinia, "Diversity through Coded Cooperation," *IEEE Trans. Wireless Commun.*, vol. 5, no. 2, pp. 283–289, Feb. 2006.
- [56] T. E. Hunter, S. Sanayei, and A. Nosratinia, "Outage Analysis of Coded Cooperation," *IEEE Trans. Inform. Theory*, vol. 52, no. 2, pp. 375–391, Feb. 2006.
- [57] E. Telatar, "Capacity of Multi-Antenna Gaussian Channels," *European Transactions on Telecommunications*, vol. 10, no. 6, pp. 585–595, Nov. 1999.
- [58] G. J. Foschini and M. J. Gans, "On Limits of Wireless Communications in a Fading Environment when Using Multiple Antennas," *Wireless Personal Communications*, vol. 6, no. 3, pp. 311–335, Mar. 1998.
- [59] E. Biglieri and G. Taricco, "Transmission and Reception with Multiple Antennas: Theoretical Foundations," *Foundations and Trends in Communications and Information Theory*, vol. 1, no. 2 (2004), pp. 183–332.
- [60] T. M. Cover and A. A. El Gamal, "Capacity Theorems for the Relay Channel," *IEEE Trans. Inform. Theory*, vol. 25, no. 5, pp. 572–584, Sept. 1979.
- [61] S. Barbarossa and G. Scutari, "Cooperative Diversity through Virtual Arrays in Multihop Networks," in *Proc. 28th IEEE International Conference on Acoustics, Speech, and Signal Processing (ICASSP 2003)*, 2003.
- [62] G. Scutari, S. Barbarossa, and D. Ludovici, "Cooperation Diversity in Multihop Wireless Networks Using Opportunistic Driven Multiple Access," in *Proc. 4th IEEE Workshop on Signal Processing Advances in Wireless Communications (SPAWC 2003)*, Rome, Italy, May 15–18, 2003.

- [63] S. Barbarossa, L. Pescosolido, D. Ludovici, L. Barbetta, and G. Scutari, “Cooperative Wireless Networks based on Distributed Space-Time Coding,” in *Proc. 1st International Workshop on Wireless Ad-hoc Networks (IWWAN 2004)*, Oulu, Finland, May 31 – June 3 2004.
- [64] S. Barbarossa and G. Scutari, “Distributed Space-Time Coding Strategies for Wideband Multihop Networks: Regenerative Vs. Non-regenerative Relays,” in *Proc. 29th IEEE International Conference on Acoustics, Speech, and Signal Processing (ICASSP 2004)*, Montreal, Quebec, Canada, May 17–21, 2004.
- [65] ———, “Distributed Space-Time Coding for Multihop Networks,” in *Proc. 2004 IEEE International Conference on Communications (ICC 2004)*, Paris, France, June 20–24, 2004.
- [66] R. U. Nabar, H. Bölcseki, and F. W. Kneubühler, “Fading Relay Channels: Performance Limits and Space–Time Signal Design,” *IEEE J. Select. Areas Commun.*, vol. 22, no. 6, pp. 1099–1109, Aug. 2004.
- [67] Gesualdo Scutari and Sergio Barbarossa, “Distributed space-time coding for regenerative relay networks,” *IEEE Trans. Wireless Commun.*, vol. 4, no. 5, pp. 2387–2399, Sept. 2005.
- [68] B. Wang, J. Zhang, and H. Høst-Madsen, “On the Capacity of MIMO Relay Channels,” *IEEE Trans. Inform. Theory*, vol. 51, no. 1, pp. 29–43, Jan. 2005.
- [69] H. Høst-Madsen and J. Zhang, “Capacity Bounds and Power Allocation for Wireless Relay Channels,” *IEEE Trans. Inform. Theory*, vol. 51, no. 6, pp. 2020–2040, June 2005.
- [70] G. Kramer, M. Gastpar, and P. Gupta, “Cooperative Strategies and Capacity Theorems for Relay Networks,” *IEEE Trans. Inform. Theory*, vol. 51, no. 1, pp. 29–43, Jan. 2005.
- [71] X. Cai, Y. Yao, and G. B. Giannakis, “Achievable Rates in Low-Power Relay Links Over Fading Channels,” *IEEE Trans. Commun.*, vol. 53, no. 1, pp. 184–194, Jan. 2005.
- [72] M. Yu and J. Li, “Amplify-Forward and Decode-Forward: The Impact of Location and Capacity Contour,” in *Proc. IEEE Military Communications Conference (MILCOM 2005)*, Atlantic City, NJ, USA, Oct. 17–20, 2005.